KRISHNAPPAN

Environment Canada | Environnement Canada

National Water Research Institute | Institut National de Recherche sur les Eaux

UNSTEADY FLOW IN MOBILE BOUNDARY CHANNELS

by

Bommanna G. Krishnappan

This manuscript has been submitted to
the Hydraulics Division, American Society of Civil Engineers
for publication and the contents are subject to change.

This copy is to provide information
prior to publication.

UNSTEADY FLOW IN MOBILE BOUNDARY CHANNELS

by

Bommanna G. Krishnappan

Environmental Hydraulics Section
Hydraulics Research Division
National Water Research Institute
Canada Centre for Inland Waters
Burlington, Ontario
April 1979

ABSTRACT

A mathematical model to predict the mean bed level, water level and discharge as a function of time and distance along a mobile boundary channel is described. The model uses the friction factor relations developed by Kishi and Kuroki which take into account the various bed forms that are found in natural streams. The sediment transport relations developed by Ackers and White which were found to be superior to most of the available methods were adopted for this model.

The model was verified in a laboratory flume by simulating degradation and aggradation processes. The experimental results compare favourably with the model predictions.

KEYWORDS

Aggradation, bed forms, channels, mathematical models, mobile boundary, unsteady flow, sediments.

SOMMAIRE

Ce document décrit un modèle mathématique visant à prévoir le niveau moyen du lit, le niveau d'eau et le débit en fonction du temps et de la distance le long d'un canal aux limites mobiles. Le modèle utilise les rapports entre les facteurs de frottement établis par Kishi et Kuroki, lesquels tiennent compte des diverses formes de lit existant dans les cours d'eau naturels. Les rapports sur le charriage de fond établis par Ackers et White et qu'on a trouvés supérieurs à la plupart des méthodes existantes, ont été adoptés pour ce modèle.

Le modèle a été vérifié dans un canal sur appuis, en laboratoire, en simulant des processus de dégradation et d'alluvionnement. Les résultats expérimentaux se rapprochent assez bien des prévisions du modèle.

MOTS CLÉS

Alluvionnement, formes de lit, canaux, modèles mathématiques, limites mobiles, écoulement non permanent.

MANAGEMENT PERSPECTIVE

In rivers, sediment reacts to the water flow. For most studies, steady, unchanging conditions are assumed. That is, for a given steady flow, a steady sediment discharge is deduced.

This model, however, permits unsteady conditions to be introduced so that the river flow and the sediment supply are both variable with time. The model provides the water elevation, the mean bed level and the sediment transport as a function of time. This is a big step forward in river modelling. Note also there are no "calibrations" or adjustments to coefficients required.

The model can be used to predict river effects owing to changes in land use or in river flow by controls or diversions. It will also permit correct interpretation of field sediment measurements.

Dr. T. M. Dick, Chief
Hydraulics Research Division
National Water Research Institute
Canada Centre for Inland Waters
May 1979

PERSPECTIVE - GESTION

Dans les cours d'eau, les sédiments réagissent à l'écoulement des eaux. On suppose, pour la plupart des études, que les conditions sont permanentes et stables. C'est-à-dire que pour un écoulement permanent donné, on déduit un débit charrié permanent.

Ce modèle permet cependant d'introduire des conditions non permanentes afin que le débit et l'apport de sédiments varient avec les temps. Le modèle fournit le niveau d'eau, le niveau moyen du lit et le charriage de fond en fonction du temps. Il s'agit d'un grand pas en avant dans le domaine de l'établissement de modèles. Remarquez également qu'il n'y a pas besoin d' "étalonnage" ou de rajustement des coefficients.

Le modèle peut être utilisé pour prévoir les effets dus aux changements d'utilisation des terres ou de débit des cours d'eau par suite de la régularisation ou de la dérivation de ceux-ci. Il permettra aussi d'interpréter correctement les mesures de sédiments prises sur place.

M. T. M. Dick, chef
Division de recherche en hydraulique
Institut national de recherche sur l'eau
Centre canadien des eaux intérieures
mai 1979

SUMMARY

A mathematical model to predict the mean bed level, water level and discharge and/or velocity as a function of time and distance along an alluvial channel is described. The roughness characteristics of alluvial stream beds are considered. The model was verified in a laboratory flume. The experimental results compare favourably with the model predictions.

Unsteady Flow in Mobile Boundary Channels

Bommanna G. Krishnappan[1]

1.0 INTRODUCTION

In the field of Water Resources Management, one is often confronted with the problem of assessing the environmental impacts of various activities of man in river basins that are likely to alter the regime of a river. These assessments require the knowledge of hydraulic parameters such as bed elevations, water surface elevations and flow velocities in mobile boundary channels when the flow rate and sediment input rates are time dependent. In the present decade, a considerable attention had been focussed on the development of numerical methods to predict these parameters.

The first attempt to develop a mathematical model for unsteady flows in mobile boundary channels was made by J. A. Cunge and N. Perdreau (5) in 1973. In their work, Cunge and Perdreau solved three one-dimensional governing equations, namely, continuity and momentum equations of liquid flow and a continuity equation of solid discharge using Finite Difference Methods. They adopted the bed-load equation proposed by Meyer-Peter and Müller (12) and a constant Strickler Coefficient to evaluate the energy slope which appears in the momentum equation. In this model, only the sediments moving in the vicinity of the bed, i.e. the bed load was considered.

In 1974, Y. H. Chen and D. B. Simons (3) reported a model to route the water and sediment in natural streams. Chen and Simons considered both bed load and suspended load and used the methods proposed by Einstein (8) and Toffaletti (15) to evaluate the total sediment transport rate. They used Manning's 'n' to compute the energy slope.

---

[1]Research Scientist, Hydraulics Research Division, National Water Research Institute, CCIW, Burlington, Ontario, Canada

In both of the above models, the influence of the bed forms on energy slope was not accounted for. In 1975, J. A. Cunge and D. B. Simons (6) developed a model taking the alluvial bed roughness into account by using theory developed by F. Engelund and E. Hansen (9) in 1967 which treats the bed forms in two regimes, namely, the lower regime consisting of dunes and ripples and the upper regime consisting of plain bed and antidunes. In this model, Cunge and Simons used the sediment transport equation that was also developed by F. Engelund and E. Hansen (9).

In 1972, Tsutomu Kishi and Kuroki (10) modified the Engelund and Hansen Method and developed friction factor equations by considering the bed forms in seven configurations, namely, dune I, dune II, transition I, transition II, flat bed, antidunes and shoot and pool. These equations agreed with the laboratory and field data better than those proposed by Engelund and Hansen. In 1973, P. Ackers and W. R. White (1) proposed a method to compute the total sediment transport rate and this method has been found to be superior to other methods developed thus far (see W. R. White, Milli, H., and Crabbe, A. D. (16)). Using the above two improved methods for predicting the friction factor and sediment transport rate in the mobile boundary channels, the present model was developed and tested in the hydraulics laboratory of the National Water Research Institute at Burlington, Ontario, Canada. A brief description of the model and its verification is presented in this paper.

2.0 GOVERNING EQUATIONS

Figure 1 shows, schematically, the longitudinal profile and a typical cross section of a stream for which the model is applicable. In the co-ordinate system shown in Figure 1, the governing equations, solved numerically in the model, are as follows:

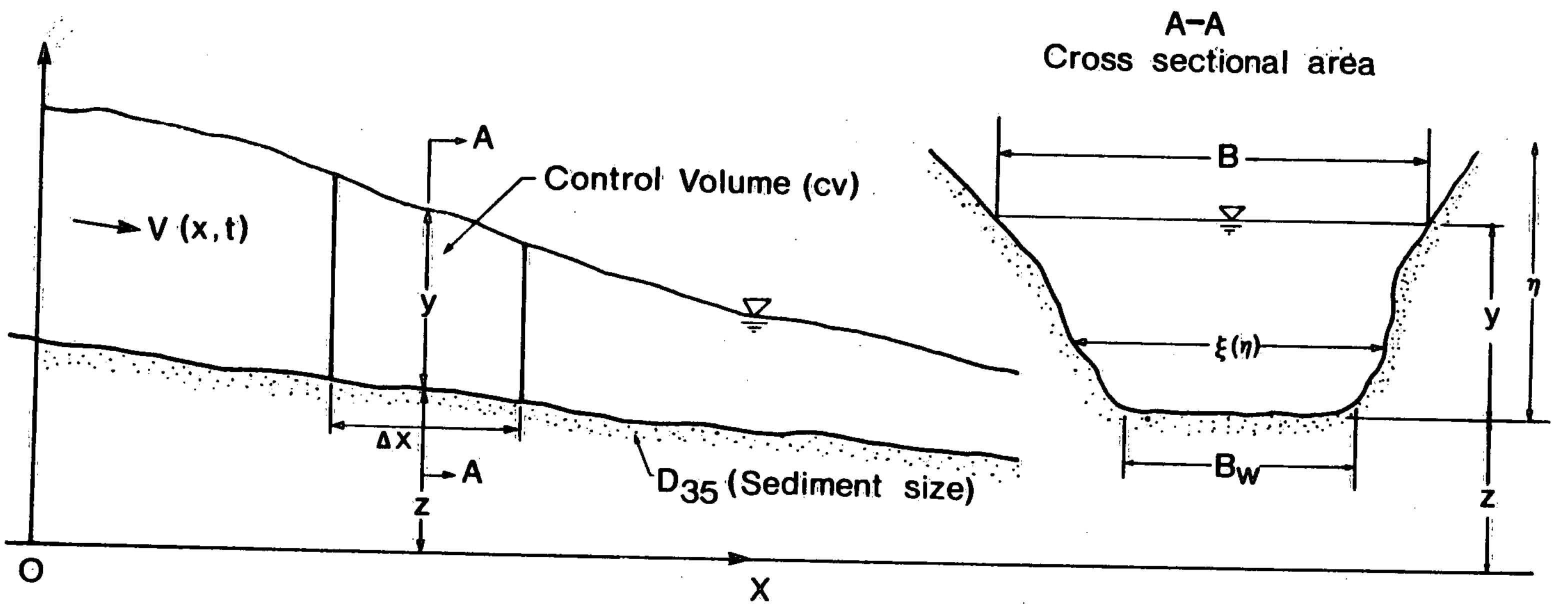

Figure 1. SCHEMATICAL REPRESENTATION OF THE LONGITUDINAL PROFILE AND A FLOW CROSS-SECTION IN A RIVER.

$$\frac{\partial Q_s}{\partial x} + P\left(\frac{\partial z}{\partial t}\right)p + BC_{av}\left(\frac{\partial y}{\partial t}\right) + A\left(\frac{\partial C_{av}}{\partial t}\right) - q_s = 0 \quad (1)$$

$$\frac{\partial Q}{\partial x} + B\left(\frac{\partial y}{\partial t}\right) + P\left(\frac{\partial z}{\partial t}\right) - q = 0 \quad (2)$$

$$\frac{\partial Q}{\partial t} + 2\frac{Q}{A}\frac{\partial Q}{\partial x} + gA\left(\frac{\partial y}{\partial x}\right) - B\frac{Q^2}{A^2}\frac{\partial y}{\partial x} = gA\left(S_o - S_f\right) + \frac{Q^2}{A^2}A_x^{\eta} \quad (3)$$

where

x	is the co-ordinate axis along the length of a stream
z	is the vertical distance between a fixed datum and the mean bed level within a control volume
y	is the vertical distance between the mean bed level within a control volume and the mean water surface elevation within the same control volume
η	is the vertical co-ordinate measured from the mean bed level within a control volume
t	is time
g	is acceleration due to gravity
Q_s	is the volumetric sediment transport rate
q_s	is the sediment input rate entering the stream laterally due to overland flow etc.
Q	is the total flow rate
q	is the lateral inflow rate into the stream
P	is the wetted perimeter
B	is the top width of the stream
A	is the flow cross-sectional area
A_x^{η}	is the rate of change of A with respect to x when η is held constant (for prismatic channels $A_x^{\eta} = 0$)

S_o is the slope of the bed within a control volume

S_f is the slope of the energy grade line

p is the volume of sediment on the bed per unit volume of bed layer

C_{av} is the average volumetric sediment concentration within a control volume.

Equation 1 is the mass balance equation for the sediment crossing the control volume. Equations 2 and 3 are flow continuity and momentum equations respectively. In deriving these equations the following assumptions were made:

1. The reach of the stream is reasonably straight so that the one-dimensional approach is valid.
2. the pressure distribution is linear in the vertical direction, i.e. hydrostatic. Therefore, the vertical accelerations are neglected.
3. The density of the sediment-water mixture is constant over the cross section.
4. The resistance equations derived for uniform and steady flows are applicable to nonuniform and unsteady flows as well.
5. The slope of the water surface is small so that the sine of the angle of inclination is equal to the angle itself.

The derivation of the governing equations was carried out in a manner analogous to Y. H. Chen (11) and the details can be found in B. G. Krishnappan and N. Snider (12).

3.0 NUMERICAL SCHEME

Following the approach adopted by Y. H. Chen (4), the term $P(\partial z/\partial t)$ in the continuity equation was dropped to uncouple the sediment mass balance equation from the continuity and momentum equations. This is justified on the grounds that the variation of the mean bed level with respect to time is slower compared to the variation of the water level with respect to time. The uncoupling of the sediment mass balance equation from the other two equations permits the continuity and momentum equations to be solved independently for one time step and then knowing the flow conditions to solve the sediment mass balance equation to improve the solution for the same time step.

3.1 Solution of Continuity and Momentum Equations

An implicit finite difference scheme developed by Priesmann (14) in 1960 was used to solve the flow continuity and momentum equations simultaneously. According to this scheme, a variable, say f, and its derivatives are discretized as follows:

$$f(x;t) = \frac{\theta}{2}\left[f_{i+1}^{j+1} + f_{i}^{j+1}\right] + \frac{1-\theta}{2}\left[f_{i+1}^{j} + f_{i}^{j}\right] \quad (4)$$

$$\frac{\partial f}{\partial x} = \theta\left[\frac{f_{i+1}^{j+1} - f_{i}^{j+1}}{\Delta x}\right] + (1-\theta)\left[\frac{f_{i+1}^{j} - f_{i}^{j}}{\Delta t}\right] \quad (5)$$

$$\frac{\partial f}{\partial t} = \frac{1}{2}\left[\frac{f_{i+1}^{j+1} - f_{i+1}^{j}}{\Delta t}\right] + \frac{1}{2}\left[\frac{f_{i}^{j+1} - f_{i}^{j}}{\Delta t}\right] \quad (6)$$

where i, j, Δx and Δt are as shown in Figure 2 and θ is a weighting coefficient that can take values between 0 and 1. When $\theta=0$, the scheme becomes fully explicit and if $\theta=1$, it is fully implicit. J. A. Cunge (7) had investigated this scheme for numerical stability and accuracy and had shown that the scheme is unconditionally stable for values of θ between 0.5 and 1 and the accuracy is second order with respect to Δx when $\theta=0.5$ and first order for any other value of θ between 0.5 and 1. Cunge observed that for $\theta=0.5$ and with small values of the

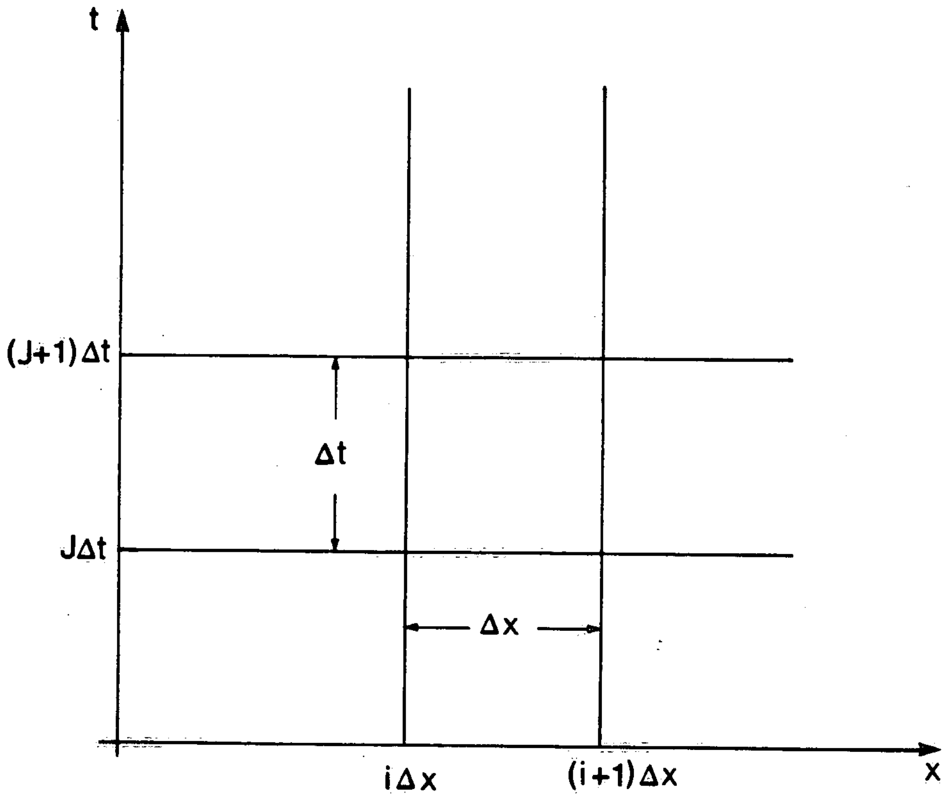

Figure 2. FINITE DIFFERENCE SCHEME

friction factor, some oscillations occurred in the solution resembling the phenomenon of numerical instability and hence suggested a practical range for θ of 0.6 to 1.0.

Expressing the value of f at $(j+1)^{th}$ time interval as a sum of the value of jth time interval and a difference Δf, i.e.

$$f^{j+1} = f^{j} + \Delta f$$

the relations (4), (5) and (6) can be rewritten as:

$$f(x;t) = \frac{1}{2}\left[\theta(\Delta f_{i+1} + \Delta f_i) + (f_{i+1} + f_i)\right] \tag{7}$$

$$\frac{\partial f}{\partial t} = \frac{1}{\Delta x}\left[\theta(\Delta f_{i+1} - \Delta f_i) + (f_{i+1} - f_i)\right] \tag{8}$$

$$\frac{\partial f}{\partial t} = \frac{1}{2\Delta t}(\Delta f_{i+1} + \Delta f_i) \tag{9}$$

The superscript for f is dropped with the understanding that f without superscript corresponds to the value of f at the jth time step. When the above expressions are substituted for the terms in continuity and momentum equations, and the second order terms like $(\Delta f/f)^2$ and $(\Delta f.\Delta g)$ are neglected the following two linear equations result:

$$a_i \, \Delta y_{i+1} + b_i \, \Delta Q_{i+1} + c_i \, \Delta y_i + d_i \, \Delta Q_i + e_i = 0 \tag{10}$$

and

$$a'_i \, \Delta y_{i+1} + b'_i \, \Delta Q_{i+1} + c'_i \, \Delta y_i + d'_i \, \Delta Q_i + e'_i = 0 \tag{11}$$

where the coefficients take the values as given by the following equations:

$$a_i = \left[\frac{B_{i+1}+B_i}{2\Delta t}\right] - \frac{2\theta}{\Delta x}\left[\frac{Q_{i+1}-Q_i}{B_{i+1}+B_i}\right]\left.\frac{dB}{dy}\right|_{i+1} + \theta\left[\frac{q_{i+1}+q_i}{B_{i+1}+B_i}\right]\left.\frac{dB}{dy}\right|_{i+1} \quad (12)$$

$$b_i = \frac{2\theta}{\Delta x} \quad (13)$$

$$c_i = \left[\frac{B_{i+1}+B_i}{2\Delta t}\right] - \frac{2\theta}{\Delta x}\left[\frac{Q_{i+1}-Q_i}{B_{i+1}+B_i}\right]\left.\frac{dB}{dy}\right|_{i} + \theta\left[\frac{q_{i+1}+q_i}{B_{i+1}+B_i}\right]\left.\frac{dB}{dy}\right|_{i} \quad (14)$$

$$d_i = -\frac{2\theta}{\Delta x} \quad (15)$$

$$e_i = \frac{2}{\Delta x}(Q_{i+1} - Q_i) - (q_{i+1} + q_i) - \theta(\Delta q_{i+1} + \Delta q_i) \quad (16)$$

$$a_i' = \frac{\theta}{\Delta x}\left\{\frac{Q_{i+1}+B_{i+1}}{A_{i+1}^2}(Q_i-Q_{i+1})\right\} + \frac{g\theta}{\Delta x}\left\{(y_{i+1}-y_i)B_{i+1}+A_{i+1}+A_i\right\} +$$

$$\frac{\theta}{2\Delta x}\left\{\left(\frac{2B_{i+1}^2Q_{i+1}^2}{A_{i+1}^3} - \left.\frac{dB}{dy}\right|_{i+1}\frac{Q_{i+1}^2}{A_{i+1}^2}\right)(y_{i+1}-y_i) - \frac{B_{i+1}Q_{i+1}^2}{A_{i+1}^2} - \frac{B_iQ_i}{A_i^2}\right\} -$$

$$\frac{g\theta}{2\Delta x}\left\{B_{i+1}(z_i-z_{i+1})\right\} + \frac{g\theta}{2}\text{const}\left(\frac{R_{i+1}}{D_{50}}\right)^m Fr_{i+1}^n\left\{B_{i+1}(m-3n) -\right.$$

$$\left.\frac{A_{i+1}}{P_{i+1}}\left.\frac{dP}{dy}\right|_{i+1}(m-n) + B_{i+1}\right\} + \theta\frac{Q_{i+1}^2B_{i+1}}{A_{i+1}^3}\left.A_{i+1}^n\right|_{i+1}$$

(17)

$$b_i' = \frac{1}{2\Delta t} + \frac{\theta}{\Delta x}\left\{\frac{Q_{i+1}}{A_{i+1}} + \frac{Q_i}{A_i} + \frac{Q_{i+1}-Q_i}{A_{i+1}}\right\} + \frac{\theta}{2\Delta x}\left\{\frac{2Q_{i+1}B_{i+1}}{A_{i+1}^2}(y_i-y_{i+1})\right\} +$$

$$g\theta.\text{const.}\left(\frac{R_{i+1}}{D_{50}}\right)^m . Fr_{i+1}^n\, n\frac{A_{i+1}}{Q_{i+1}} - \theta\frac{Q_{i+1}}{A_{i+1}^2}\left.A_x^n\right|_{i+1}$$

(18)

$$c'_i = \frac{\theta}{\Delta x}\left\{\frac{Q_i B_i}{A_i^2}(Q_i - Q_{i+1})\right\} + \frac{g\theta}{2\Delta x}\left\{(y_{i+1}-y_i) \quad B_i - A_{i+1} - A_i\right\} +$$

$$\frac{\theta}{2\Delta x}\left\{\left(\frac{2B_i^2 Q_i^2}{A_i^3} - \left.\frac{dB}{dy}\right|_i \frac{Q_i^2}{A_i^2}\right)(y_{i+1} - y_i) + \frac{B_{i+1}\, Q_{i+1}^2}{A_{i+1}^2} + \frac{B_i\, Q_i^2}{A_i^2}\right\} -$$

$$\frac{g\theta}{2\Delta x}\left\{B_i\,(z_i - z_{i+1})\right\} + \frac{g\theta}{2}.\,\text{const.}\left(\frac{R_i}{D_{50}}\right)^m . Fr_i^n \left\{B_i\,(m-3n) -\right.$$

$$\left.\frac{A_i}{P_i}\left.\frac{dP}{dy}\right|_i (m-n) + B_i\right\} + \theta\,\frac{Q_i^2 B_i}{A_i^3}\left.\quad A_x^\eta\right|_i$$

(19)

$$d'_i = \frac{1}{2\Delta t} + \frac{\theta}{\Delta x}\left\{\frac{(Q_{i+1} - Q_i)}{A_i} - \frac{Q_{i+1}}{A_{i+1}} - \frac{Q_i}{A_i}\right\} + \frac{\theta}{2\Delta x}\left\{\frac{2Q_i\, B_i}{A_i^2}\quad (y_i - y_{i+1})\right\} +$$

$$g\theta.\text{const.}\left(\frac{R_i}{D_{50}}\right)^m \quad Fr_i^n \quad n\,\frac{A_i}{Q_i} - \theta\,\frac{Q_i}{A_i^2}\left.\quad A_x^\eta\right|_i$$

(20)

$$e'_i = \frac{1}{\Delta x}\left\{(Q_{i+1} - Q_i)\left(\frac{Q_{i+1}}{A_{i+1}} + \frac{Q_i}{A_i}\right)\right\} + \frac{g}{2\Delta x}\left\{(A_{i+1} + A_i)\,(y_{i+1} - y_i)\right\} +$$

$$\frac{1}{2\Delta x}\left\{\left(\frac{B_{i+1}\, Q_{i+1}^2}{A_{i+1}^2} + \frac{B_i\, Q_i^2}{A_i^2}\right)(y_i - y_{i+1})\right\} + \frac{g}{2\Delta x}\left\{(A_{i+1} + A_i)(z_{i+1} - z_i)\right\} +$$

$$\frac{g}{2}.\text{const.}\left(\frac{R_{i+1}}{D_{50}}\right)^m . Fr_{i+1}^n \quad A_{i+1} + \frac{g}{2}.\text{const.}\left(\frac{R_i}{D_{50}}\right)^m Fr^n \quad A_i \; -$$

$$\frac{1}{2}.\frac{Q_{i+1}^2}{A_{i+1}^2}\left.\quad A_x^\eta\right|_{i+1} - \frac{1}{2}\,\frac{Q_i^2}{A_i^2}\left.\quad A_x^\eta\right|_i$$

(21)

In the derivation of Equations (17) to (21), the slope of the energy grade line S_f was evaluated using the friction factor equations developed by Kishi and Kuroki as

$$S_f = \text{const.} \left(\frac{R}{D_{50}} \right)^m . Fr^n \tag{22}$$

where const, m and n are friction parameters which take different values depending on the type of the bed form. D_{50} is the median size of the sediment mixture and Fr is the square of the Froude Number, i.e.

$$Fr = \frac{Q^2}{A^2 gR} \tag{23}$$

According to Kishi and Kuroki, the friction coefficient C defined as the ratio of the average velocity v and the shear velocity v_*, i.e. $C = v/v_*$, for different bed configurations was given as follows:

(i) for dune I, $C = 2.40 Z^{1/6} Y^{-1/3}$ (24)

(ii) for dune II, $C = 8.9$ (25)

(iii) for transition I, $C = 1.10 \times 10^6 Z^{-3/2} Y^3$ (26)

(iv) for flat bed, $C = 6.9 Z^{1/6}$ (27)

and (v) for antidunes, $C = 2.8 Z^{3/10} Y^{-1/3}$ (28)

where the symbols Z and Y stand for the following dimensionless groups consisting of flow and sediment characteristic parameters:

i.e
$$Z = \frac{R}{D_{50}}$$
$$Y = \frac{\gamma}{\gamma_s} \cdot \frac{v_*^2}{g\, D_{50}} \qquad (29)$$

γ is the specific weight of fluid and γ_s is the submerged specific weight of the sediment particles.

The criteria for the occurrence of the various bed configurations were stated as follows:

(i)	for dune I,	$Y < 0.02\, Z^{1/2}$	(30)
(ii)	for dune II,	$Y = 0.02\, Z^{1/2}$	(31)
(iii)	for transition I,	$0.02\, Z^{1/2} < Y < 0.02\, Z^{5/9}$	(32)
(iv)	for flat bed,	$0.02\, Z^{5/9} < Y < 0.07\, Z^{2/5}$	(33)
(v)	for antidunes,	$Y > 0.07\, Z^{2/5}$	(34)

The agreement between the formulae of Kishi and Kuroki and their experimental data can be seen in Figure 3. The friction parameters const, m and n can be evaluated from Equations 24 to 28 as follows:

(i)	for dune I,	$const=(\gamma/\gamma_s)^2/191$;	$m=1.00$;	$n=3$	(35)
(ii)	for dune II,	$const=(1/8.9)^2$;	$m=0.00$;	$n=1$	(36)
(iii)	for transition I,	$const=(1/53.43)(\gamma/\gamma_s)^{-6/7}$;	$m=-3/7$;	$n=1/7$	(37)
(iv)	for flat bed,	$const=(1/47.6)$;	$m=-1/3$;	$n=1$	(38)
(v)	for antidunes,	$const=(\gamma/\gamma_s)^2/482$;	$m=1/5$;	$n=3$	(39)

Evaluating the friction parameters const, m and n using the above equations, the equations 10 and 11 can be applied to all the N grid points along the length of a river reach to obtain a system of two (N-1) linear equation involving 2N unknowns, namely $\Delta Q_1, \Delta Q_2, \ldots \Delta Q_N$ and $\Delta y_1, \Delta y_2 \ldots \Delta y_N$. With

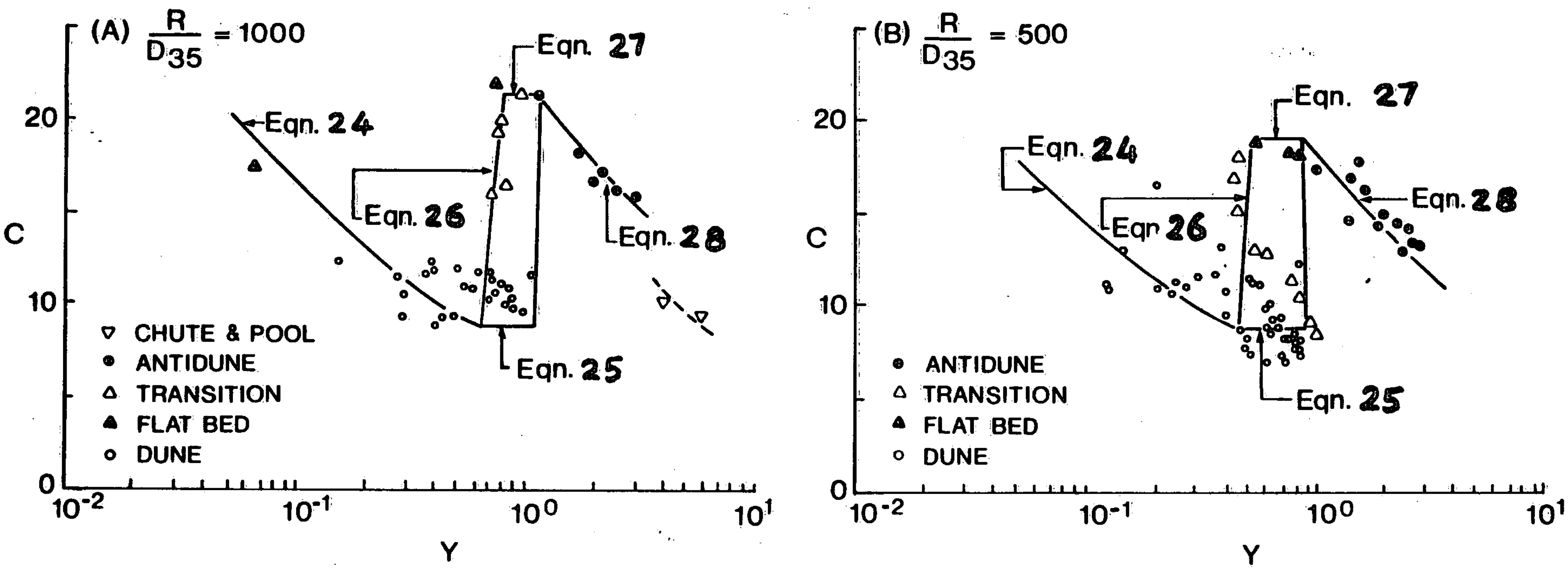

Figure 3. COMPARISON OF CALCULATED VALUES OF C WITH EXPERIMENTS (after Kishi & Kuroki)

two known boundary conditions (one at the upstream boundary and the other at the downstream boundary, for subcritical flows) the number of equations matches the number of unknowns and hence the system of equations can be solved using any one of the available standard methods. In this work, a "Double Sweep Method" was adopted. A detailed description of the method for a variety of boundary condition specifications can be found in reference (7).

After solving for ΔQ_1, ΔQ_2, ... ΔQ_N and Δy_1, Δy_2... Δy_N, the values of Q and y at the end of the first time step can be obtained by simply adding these values to the initial values for Q and y. Knowing the values of Q and y at the beginning of the first time step and at the end of the first time step, the sediment mass balance equation can be solved to compute the change in the mean bed levels Δz during the first time step as follows.

3.2 Solution of Sediment Mass Balance Equation

The sediment mass balance equation, i.e. Equation 1, can be rearranged as:

$$\frac{\partial z}{\partial t} = \frac{1}{P} \left\{ \frac{\partial Q_s}{\partial x} + B\, C_{av} \frac{\partial y}{\partial t} + \frac{\partial C_{av}}{\partial t} - q_s \right\} \cdot \frac{1}{p} \qquad (40)$$

substituting Equation (7) to (9) in the above equation, the mean bed level change Δz can be expressed as:

$$\Delta z_{i+1} = \left(\frac{\Delta t}{p}\right) \left[\theta \left(\left.\frac{dP}{dy}\right|_{i+1} \Delta y_{i+1} + \left.\frac{dP}{dy}\right|_{i} \Delta y_i \right) + \left(P_{i+1} + P_i \right) \right]^{-1}$$

$$\left[\frac{1}{\Delta x} \left\{ \theta \left(\Delta Q_{s_{i+1}} - \Delta Q_{s_i} \right) + \left(Q_{s_{i+1}} - Q_{s_i} \right) \right\} + \frac{1}{2} \left\{ \theta \left(\Delta (B C_{av})_{i+1} + \Delta (B C_{av})_i \right) + \right.\right.$$

$$(B\,C_{av})_{i+1} + (B\,C_{av})_i \left\{ \frac{(\Delta y_{i+1} + \Delta y_i)}{2\Delta t} \right\} + \frac{1}{2} \left\{ \theta\,(\Delta A_{i+1} + \Delta A_i) + (A_{i+1} + A_i) \right\} \left\{ \frac{1}{2\Delta t} (\Delta C_{av_{i+1}} + \Delta C_{av_i}) \right\} - \frac{1}{2} \left\{ \theta\,(\Delta q_{s_{i+1}} + \Delta q_{s_i}) + (q_{s_{i+1}} + q_{s_i}) \right\} - \Delta z_i \qquad (41)$$

From the boundary condition for the bed elevation at the upstream, the quantity Δz_i can be evaluated as:

$$\Delta z_1 = z_1^{j+1} - z_1^{j} \qquad (42)$$

The sediment transport rate Q_s and the average concentration C_{av} can be predicted knowing the flow conditions at the beginning of the first time step and at the end of the first time step and knowing the sediment characteristics using any one of the methods available in the literature. For reasons indicated earlier, the method proposed by Ackers and White (2) was adopted for the present model. Evaluating Δz_1 from the upstream boundary condition for the mean bed level and Q_s and C_{av} using the method of Ackers and White, the change of mean bed level during the first time step can be computed using Equation (41). Knowing the initial mean bed level at the beginning of the first time step, the mean bed level at the end of the first time step is obtained as

$$z^{j+1} = z^{j} + \Delta z \qquad (43)$$

After computing z_{i+1}^{j+1} and before proceeding to the next time step, the flow depth y solved from the continuity and momentum equations was adjusted for the change in the mean bed level as:

$$\bar{y}^{j+1} = y^{j+1} - \Delta z \tag{44}$$

where $\bar{y}^{j+1}$ is the corrected flow depth after considering the sediment mass balance equation. It is assumed that the computed flow rate Q^{j+1} does not change significantly due to the consideration of sediment mass balance equation. However, the change in the flow depth will result in changes in the flow cross-sectional areas A^{j+1}, wetted perimeters P^{j+1}, hydraulic radii R^{j+1}, the widths B^{j+1} and the friction parameters, const, m and n. Using the new values for the above parameters, the flow continuity and momentum equations are solved to correct the solution. This process is continued until the required number of time steps is reached. A flow chart describing the above computational steps is shown in Figure 4. The subroutine "GEOM" calculates the geometric parameters A, P, R, B, A_x^{η}, dB/dy, dP/dy. The subroutine "FRICT" calculates the friction parameters, const, m and n. The subroutine "SEDI" computes the sediment transport rate Q_s and the average concentration C_{av}.

4.0 LABORATORY VERIFICATION OF THE MODEL

The model was tested in the Hydraulics Laboratory of the National Water Research Institute at Burlington, Ontario, Canada. The sediment transport flume used for this purpose is 75 ft (22.9 m) long and 6.6 ft (2 m) wide. The slope of the flume bed can be varied anywhere between +0.6% to -1.0%. The flume is equipped with a sediment feeder at the upstream and sediment traps

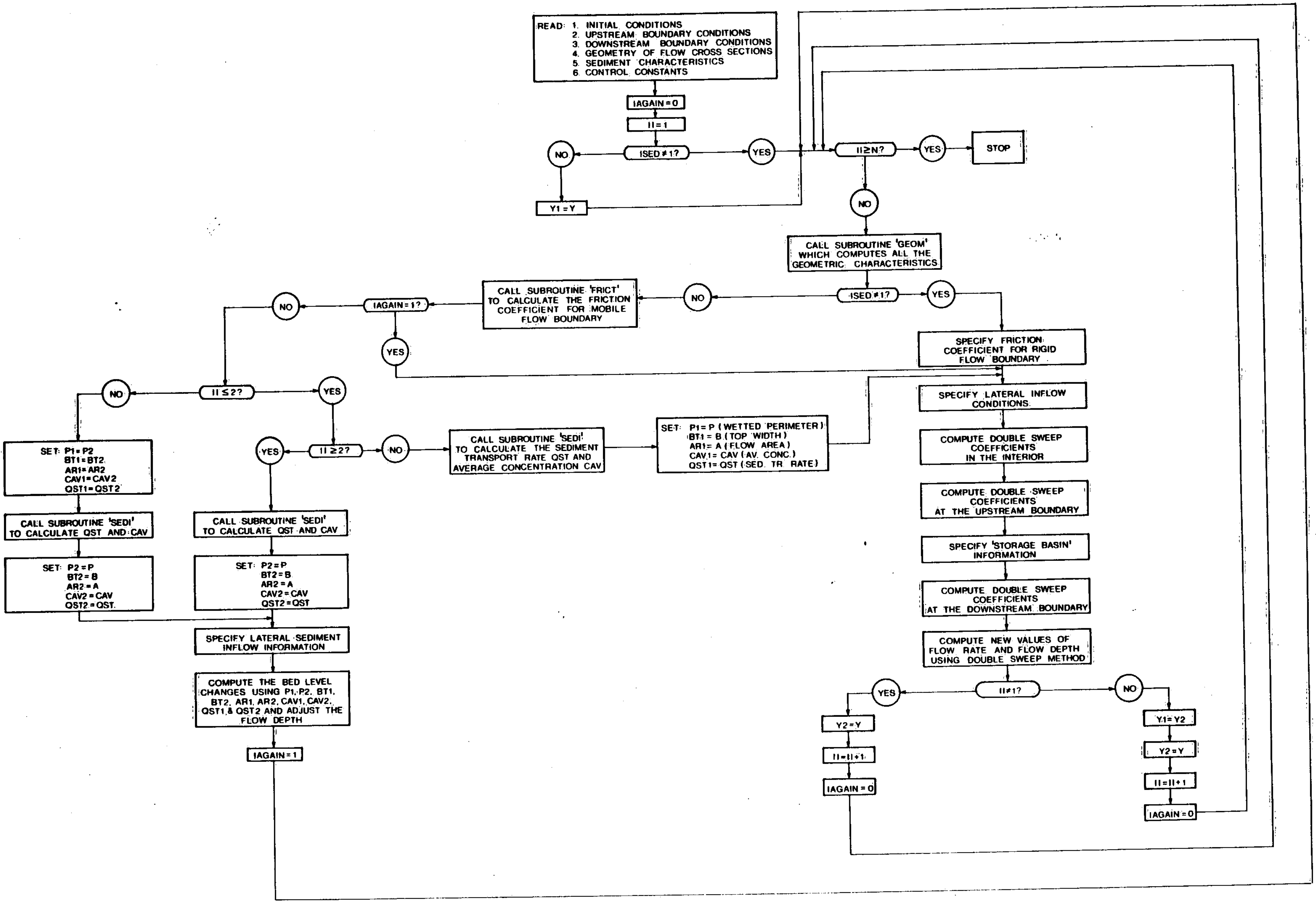

FIGURE 4. FLOW CHART FOR THE MATHEMATICAL MODEL

downstream. A carriage for the instruments, driven by an electric motor, traverses along the length of the flume at three different speeds of 2 in/sec (5 cm/s), 4 in/sec (10 cm/s) and 12 in/sec (30 cm/s). The water supply for the flume is from a constant head tank. Water enters the flume through an inlet pipe, a diffuser and a head box fitted with baffles and flow straighteners. The flow rate is controlled by a butterfly valve fitted to the inlet pipe and is measured using an "annubar" flow meter. A general view of the flume arrangement is shown in the photograph in Figure 5.

The instruments mounted on the carriage include a water level indicator and a bed level indicator. The water level indicator is a conductivity type, consisting of a point gauge, which follows the water level by maintaining contact with the water surface at all times. The bed level indicator is an optical instrument and follows the bed contour by maintaining a constant gap between the bed and its tip. The signals from these indictors are plotted on a XYY' recorder. The water level is supplied to the Y channel and the bed level to the Y' channel. The distance travelled by the carriage is fed into the X channel. A view of the instruments mounted on the carriage is shown in the photograph in Figure 6.

Altogether six runs were made in the flume. Table 1 summarizes the nature of the various runs carried out. In the first two runs, the degradation process was simulated. In these runs, the water supply rate was kept constant and the bed was allowed to scour from a transition point. A plywood false bottom was constructed to cover a part of the flume of length 13.1 ft (4 m) from the head box. The remaining length was covered with a reasonably uniform sand of size 1.2 mm. The false bottom was coated with a layer of sand to produce the same skin friction characteristics as that of the sand bottom. The initial slopes and water supply rates are given in Table 1.

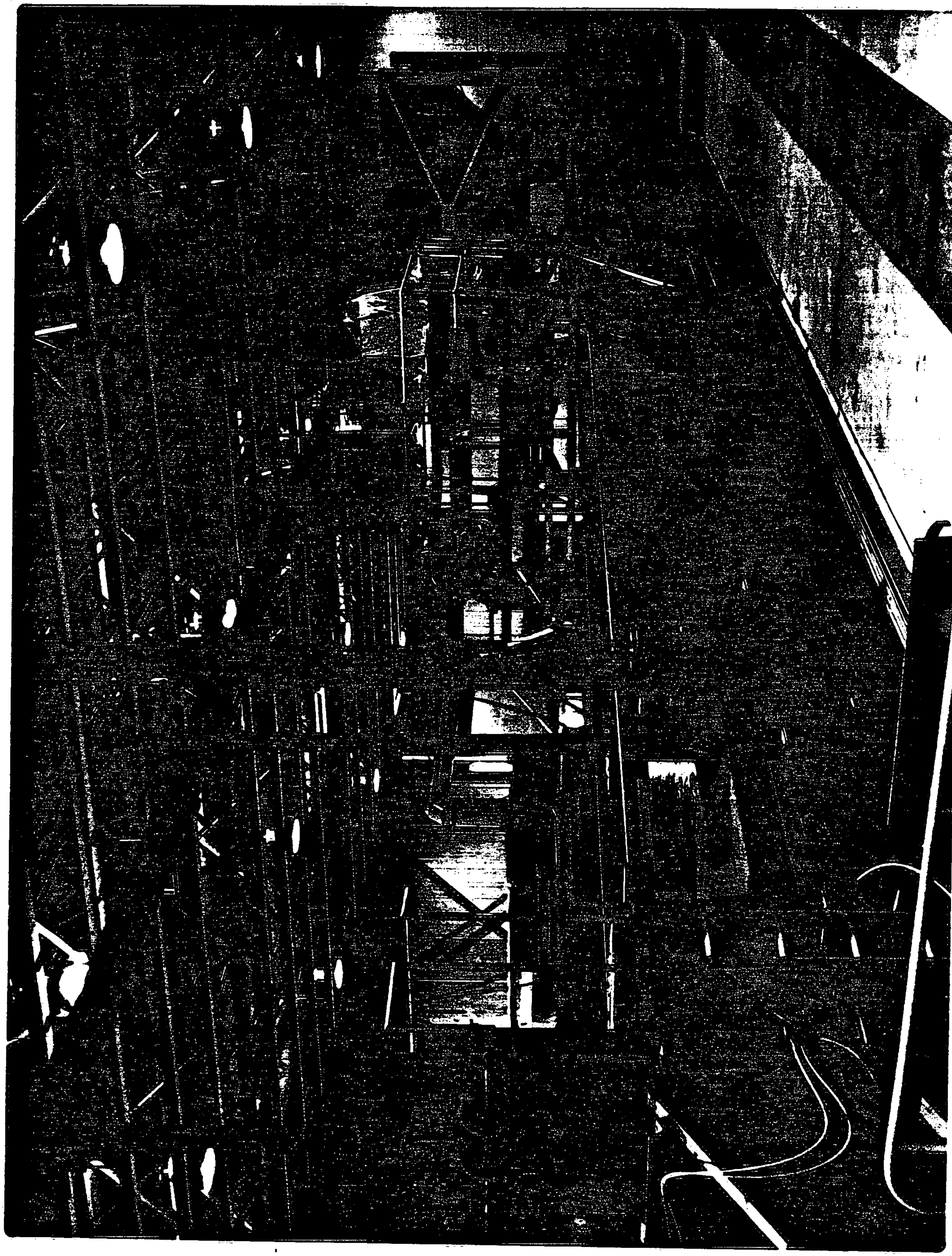

Fig. 5
Krishnappan

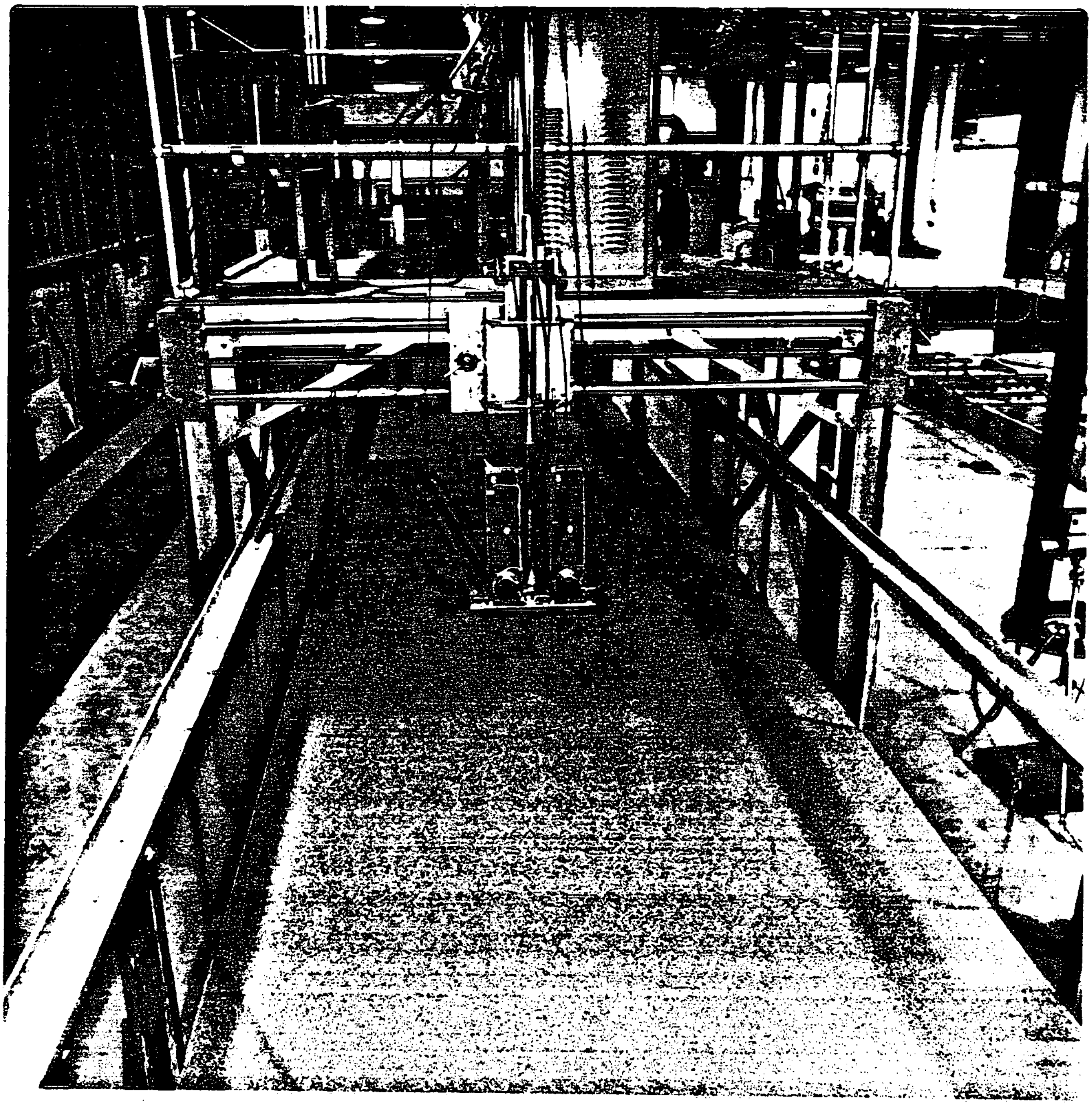

Fig. 6
Krishnappan

TABLE 1 SUMMARY OF THE EXPERIMENTAL CONDITIONS

Run No.	Water Supply Rate at Flume Entrance	Sediment Supply Rate at Flume Entrance	Initial bed Slope	Nature of the Sedimentation Process Simulated
1	Constant at 0.149 m^3/s	0	1/1000	Degradation
2	Constant at 0.186 m^3/s	0	1/667	Degradation
3	Constant at 0.193 m^3/s	Constant at 0.023 kg/s	1/2000	Aggradation
4	Constant at 0.193 m^3/s	Constant at 0.079 kg/s	1/2000	Aggradation
5	Varying as in figure 9	Constant at 0.06 kg/s	1/1000	Degradation + Aggradation
6	Varying as in figure 10	Constant at 0.06 kg/s	1/1000	Degradation + Aggradation

The tractive force of the flow established in both runs were of such magnitude that the flows were capable of transporting sediment. As the sediment scour immediately downstream of the transition occurred, the bed and water level profiles were recorded by traversing the bed and water level indicators along the length of the flume at various intervals of time. Figures 7a to 7g show the measured profiles as solid lines for run 1. Using the water level and bed level profiles in Figure 7a asthe initial conditions and the constant flow rate at the upstream and the measured depth downstream as boundary conditions, the model predictions were made for the bed and water level and are plotted as dots in Figures 7b to 7g. In the application of this model there is no need to adjust any coefficients and hence there is no need for the calibration of the model. It can be seen from these figures that the model predicts the scour depths reasonably well. Similar figures for run 2 are not shown here due to space limitation but they also exhibit similar agreement as for run no. 1. It can be seen that the mean energy slope decreases gradually and the scour depth approaches an equilibrium value. These results are in qualitative agreement with the experimental measurements of S. Bhamidipaty and H. W. Shen (2) who studied the processes of degradation and aggradation in a laboratory flume.

Runs 3 and 4 simulated the process of aggradation. In these runs, first, flows just capable of moving the sediment were established, then the sediment was fed at the upstream at a rate much higher than the transport capacity of the flow. The sediment supply rates for run 3 and 4 were .05 lbs/sec (.023 kg/s) and 0.17 lbs/sec (0.079 kg/s) respectively.

The oversupply of sediment at the flume entrance resulted in the sediment deposition and the aggradation of the stream bed. Because of this, the tractive force of the flow in the vicinity increased and consequently the downward movement of the aggradation took place. The bed and water levels monitored at various instants of time are given in Figures 8a to 8c as continuous lines for run 3. Using the bed and water levels given in Figure 8a as initial

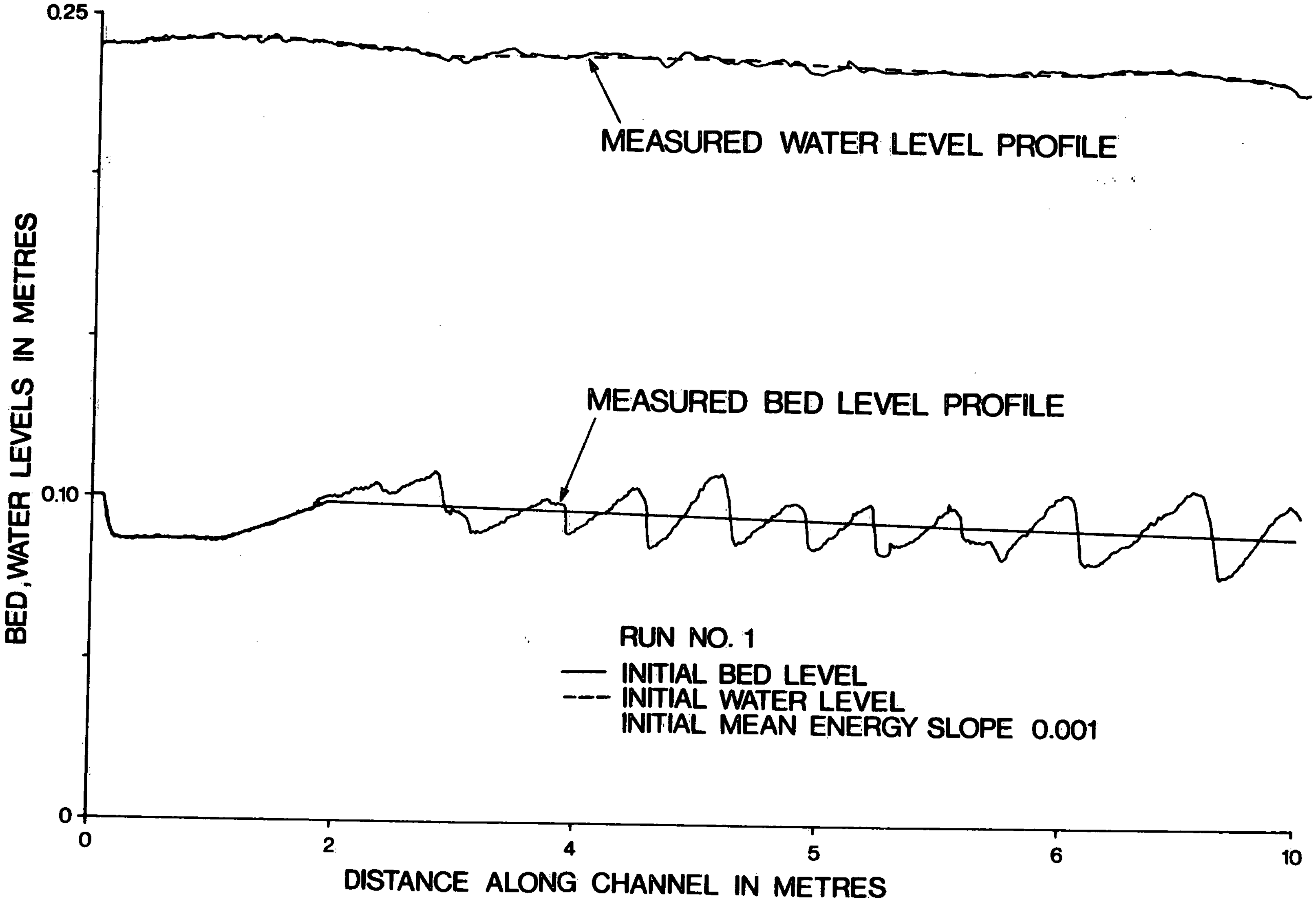

FIGURE 7a. MEAN BED LEVEL AND WATER LEVEL PROFILES USED AS INPUTS INTO THE MODEL FOR RUN #1

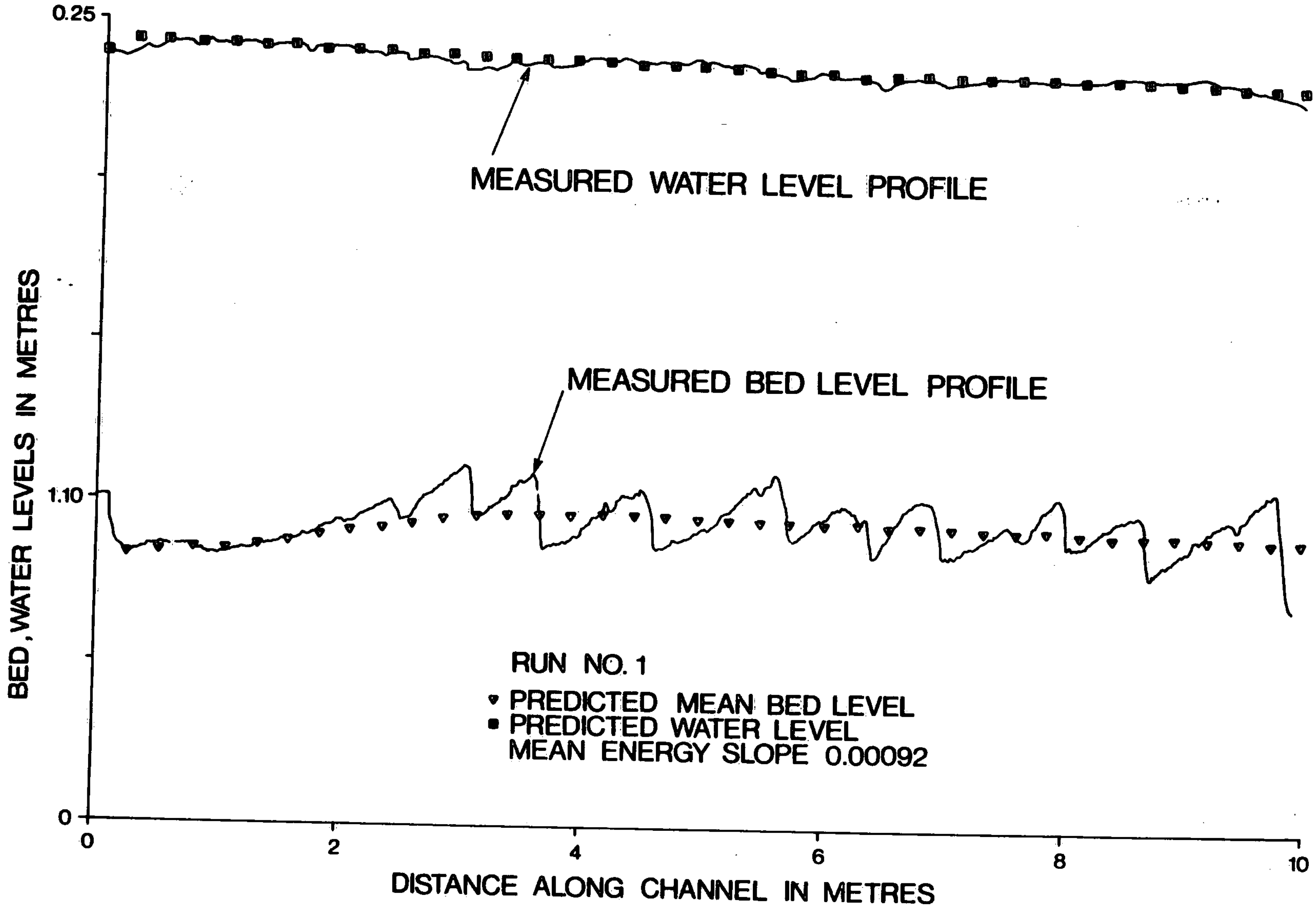

FIGURE 7b. COMPARISON OF MODEL PREDICTIONS WITH LABORATORY MEASUREMENTS FOR AN ELAPSED TIME OF ½ HOUR

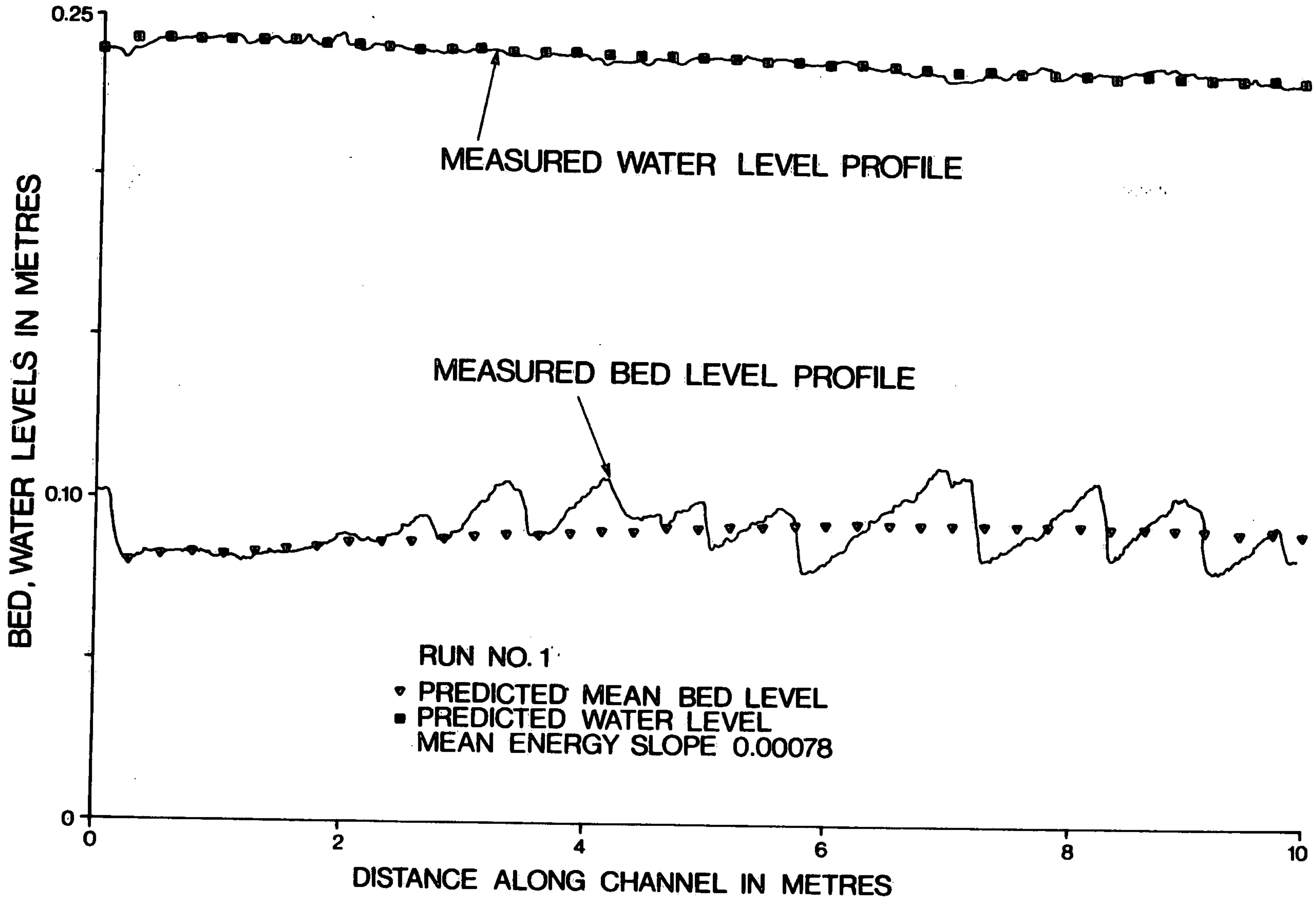

FIGURE 7c. COMPARISON OF MODEL PREDICTIONS WITH LABORATORY MEASUREMENTS FOR AN ELAPSED TIME OF 1½ HOURS

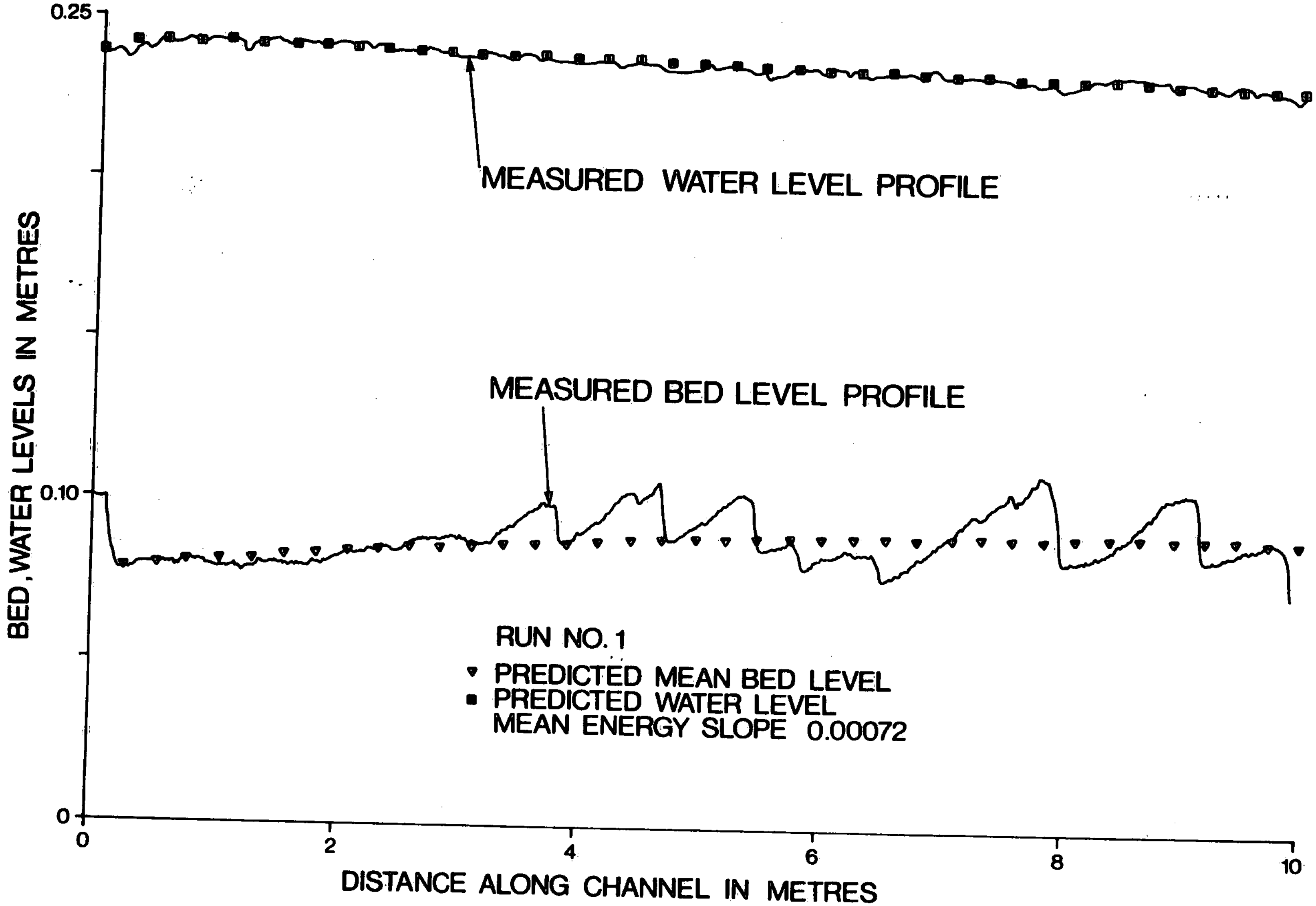

FIGURE 7d. COMPARISON OF MODEL PREDICTIONS WITH LABORATORY MEASUREMENTS FOR AN ELAPSED TIME OF 2 HOURS

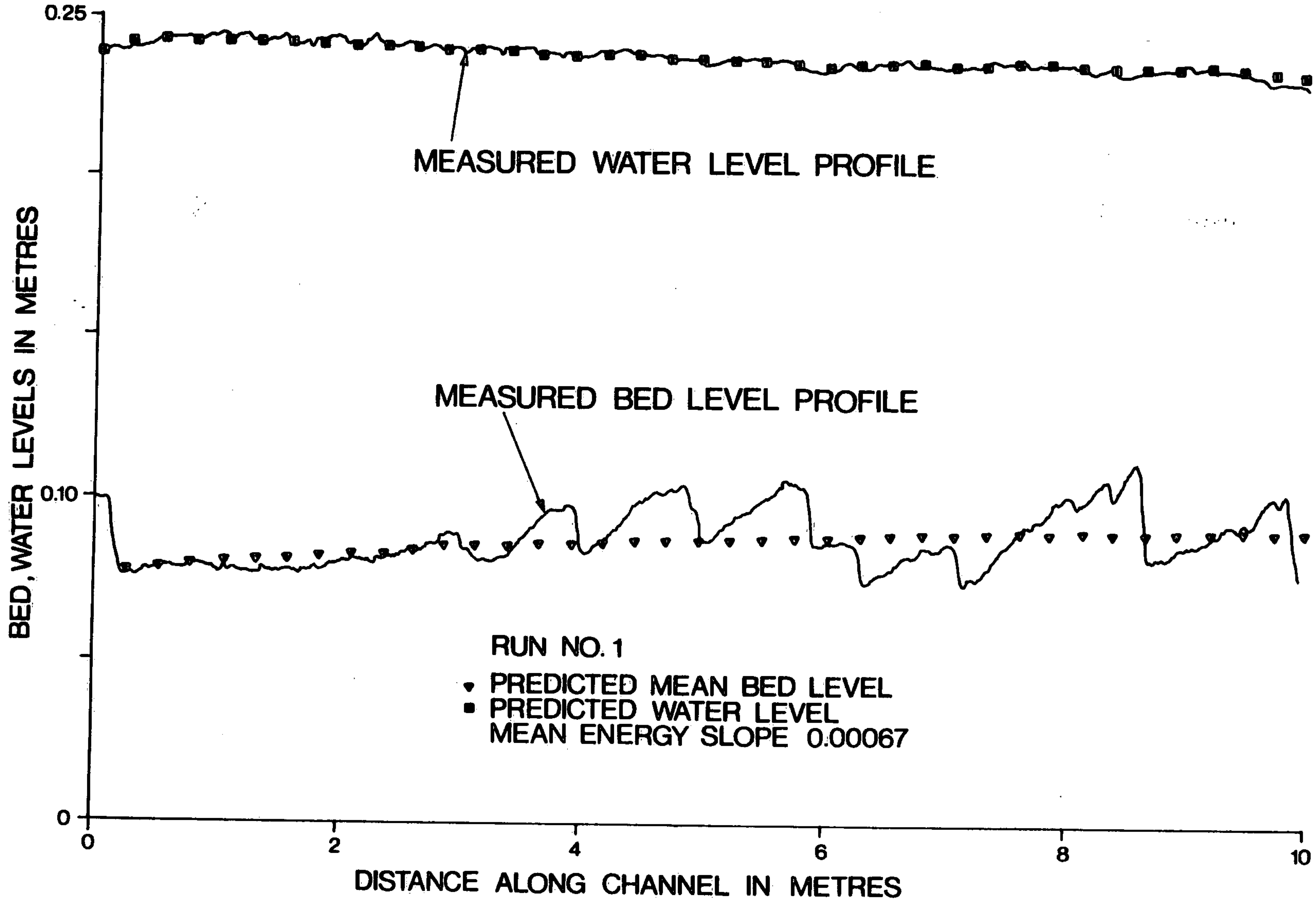

FIGURE 7e. COMPARISON OF MODEL PREDICTIONS WITH LABORATORY MEASUREMENTS FOR AN ELAPSED TIME OF 2 ½ HOURS

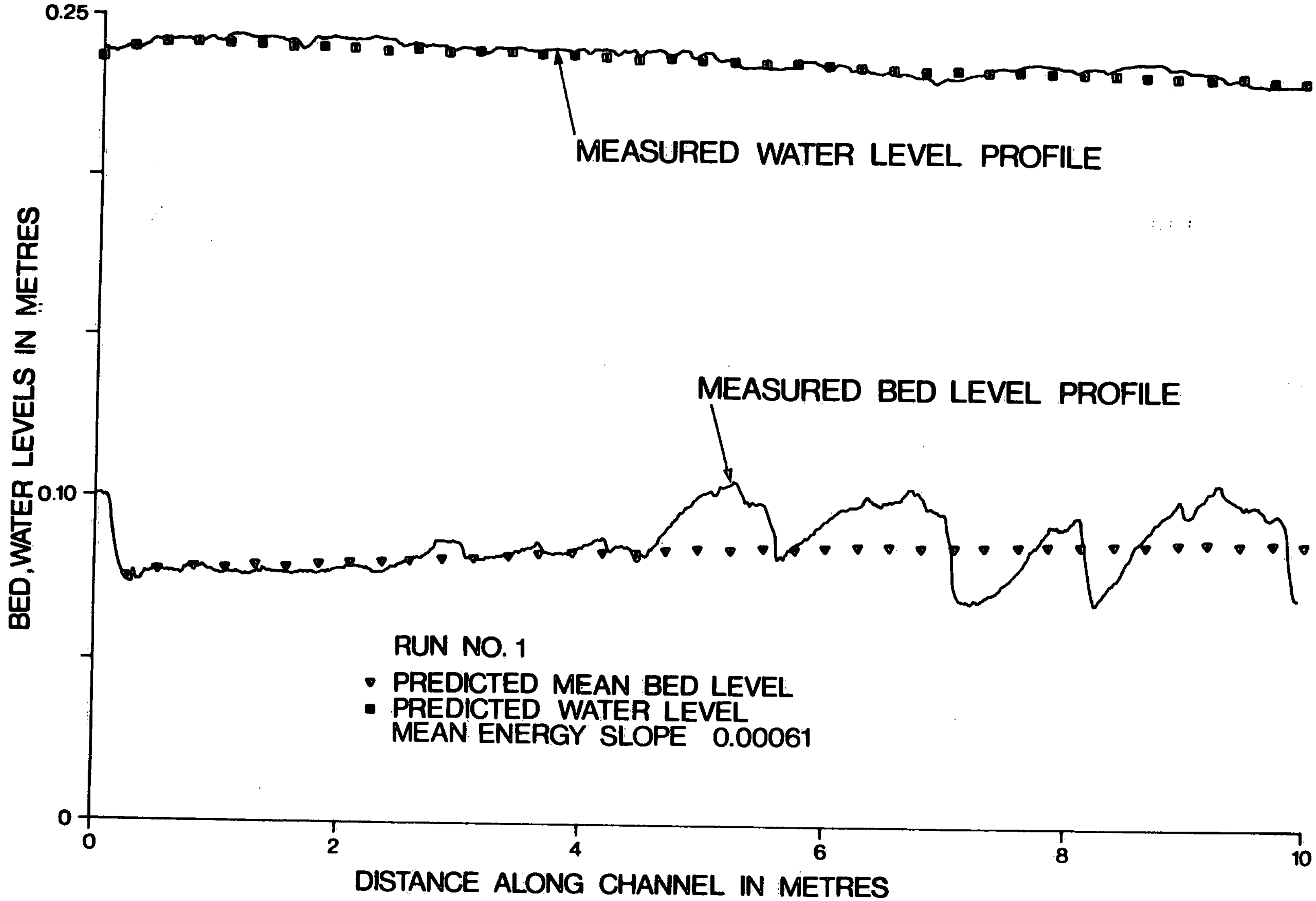

FIGURE 7f. COMPARISON OF MODEL PREDICTIONS WITH LABORATORY MEASUREMENTS FOR AN ELAPSED TIME OF 3½ HOURS

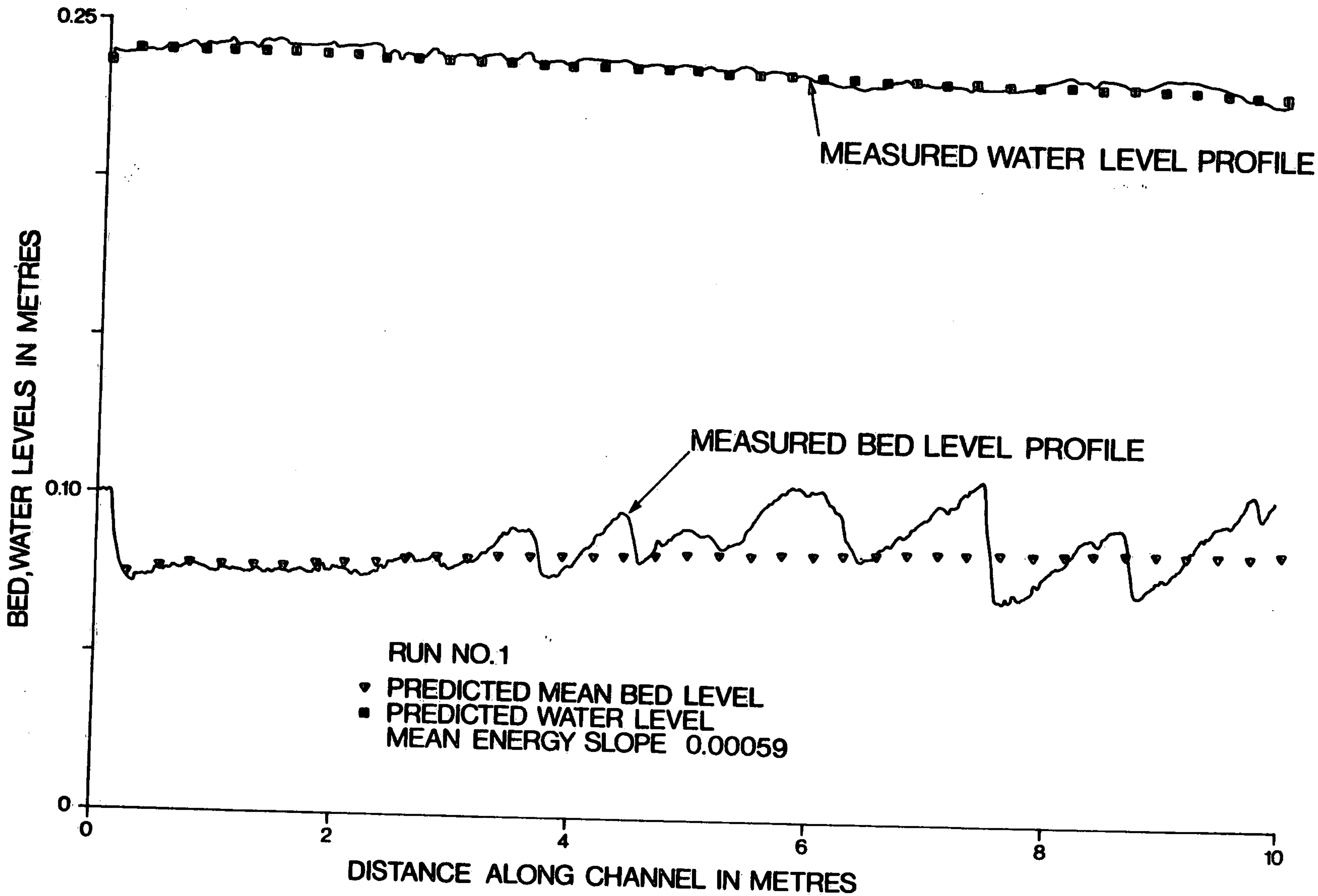

FIGURE 7g. COMPARISON OF MODEL PREDICTIONS WITH LABORATORY MEASUREMENTS FOR AN ELAPSED TIME OF 4 HOURS

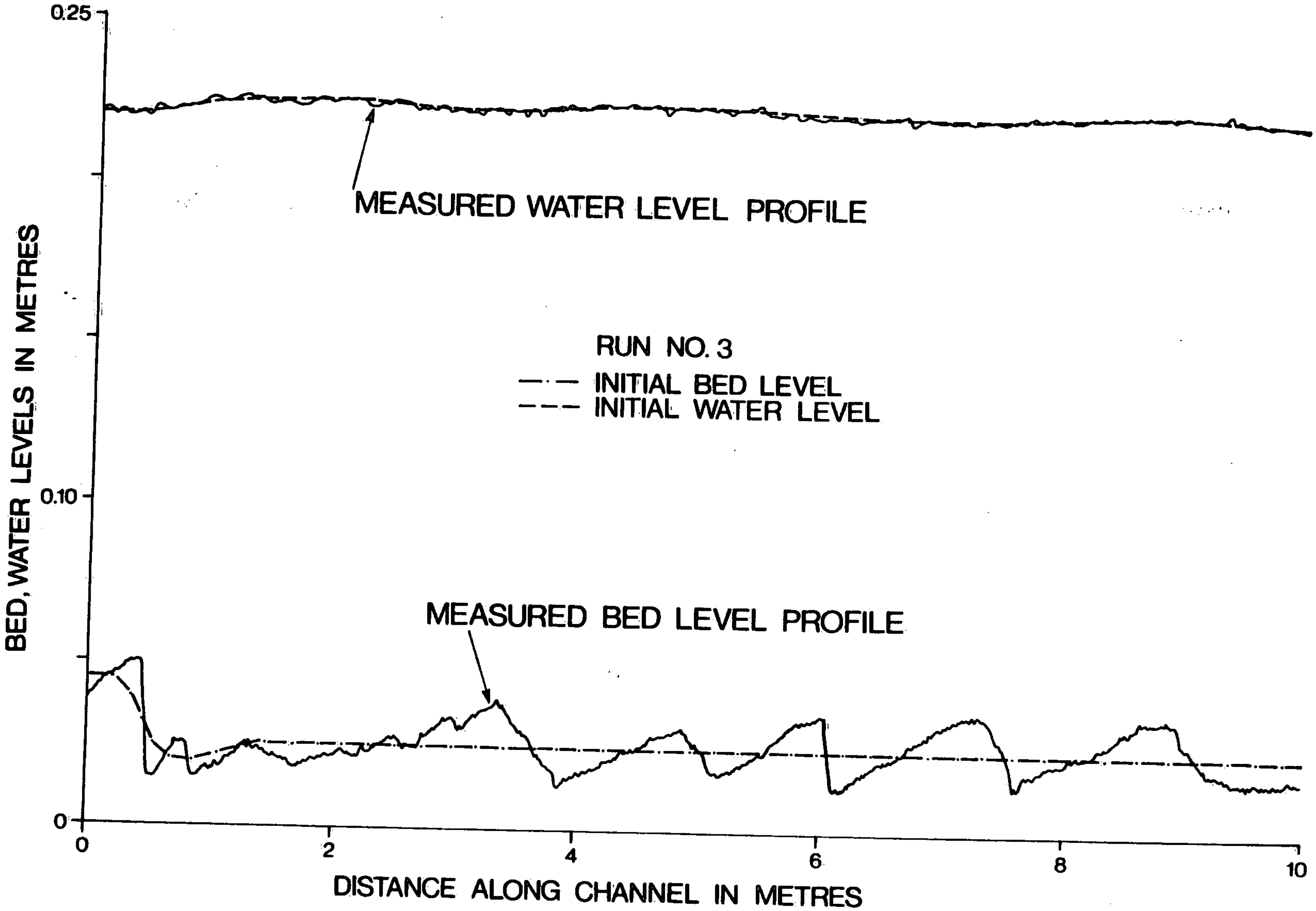

FIGURE 8a. INITIAL BED AND WATER LEVELS USED AS INPUT TO MODEL FOR RUN NO. 3

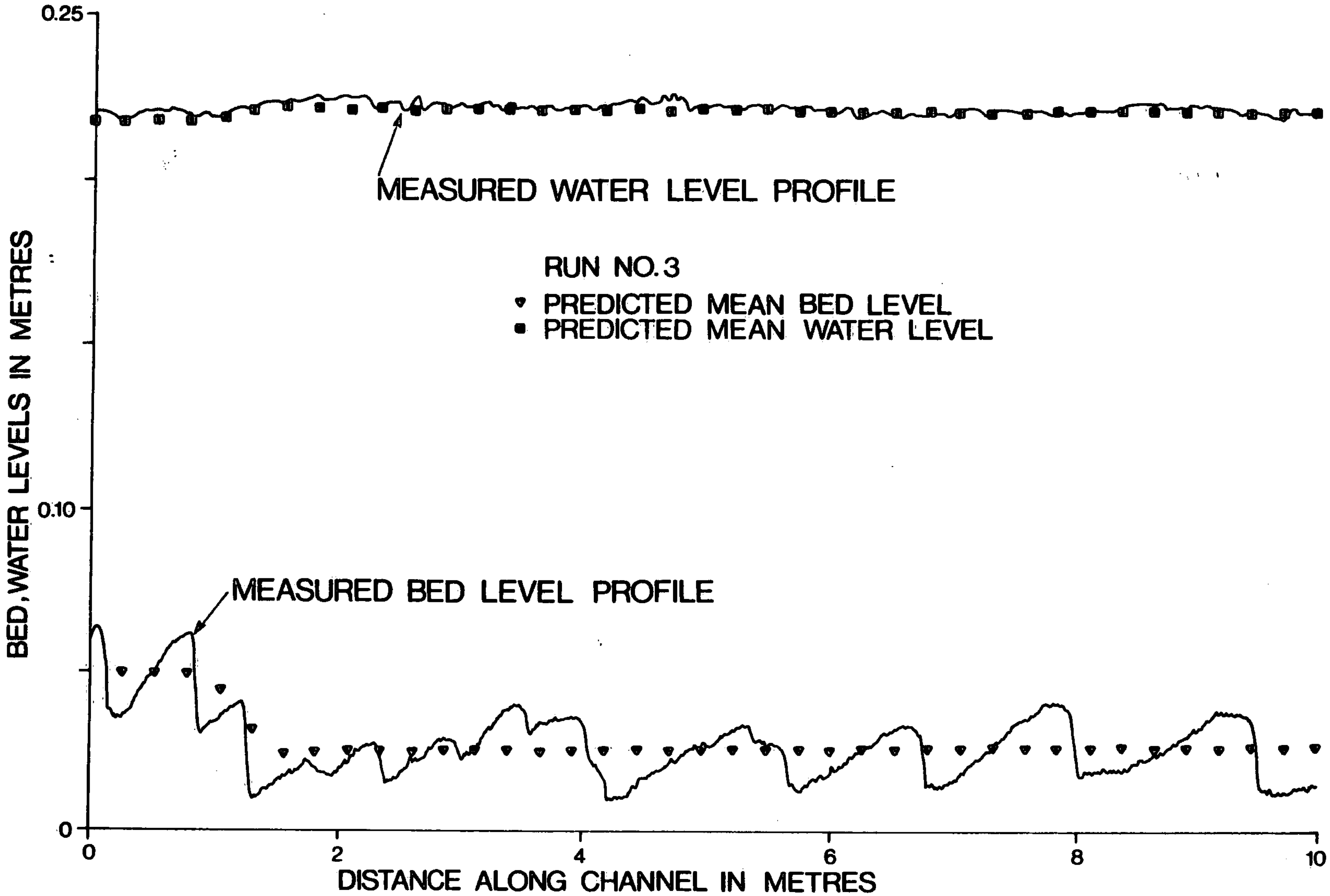

FIGURE 8b. COMPARISON OF MODEL PREDICTIONS WITH LABORATORY MEASUREMENTS FOR AN ELAPSED TIME OF 1 HOUR

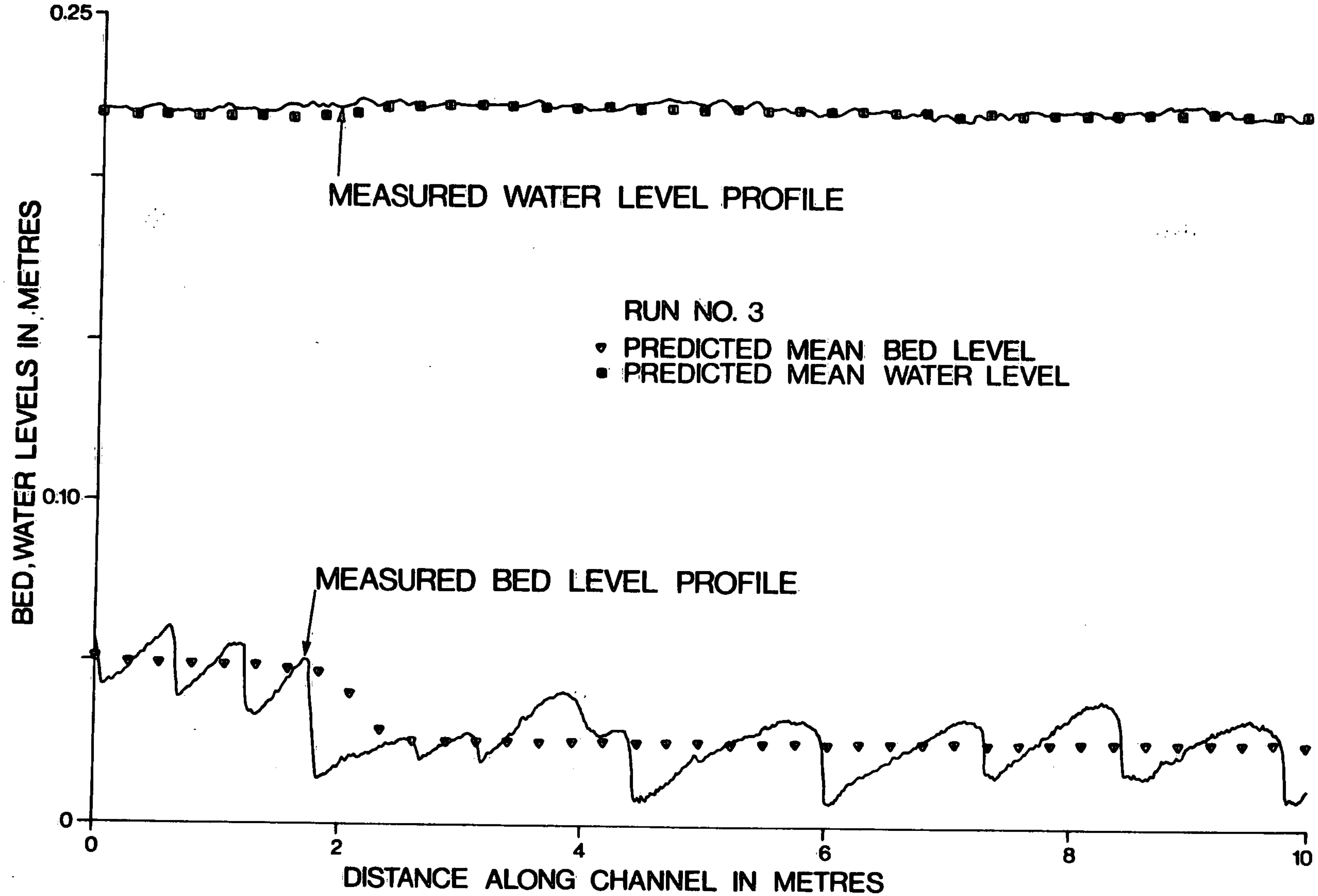

FIGURE 8c. COMPARISON OF MODEL PREDICTIONS WITH LABORATORY MEASUREMENTS FOR AN ELAPSED TIME OF 2 HOURS

conditions, the model predictions were carried out and are plotted in Figures 8b to 8c as dots. It can be seen from these figures that the movement of the aggradation agrees with the model prediction reasonably well. Again, the figures for run 4 are not shown here. The behaviour of the aggraded bed was in agreement with that observed by Bhamidipaty and Shen in their experiments.

In runs 5 and 6, the sediment supply rate was held constant at .13 lb/sec (0.06 kg/s) and in water supply rates at the flume entrance were changed in steps as shown in Figures 9 and 10 respectively. In run 5, the water supply rate changed from a higher value to a lower value and then back to a higher value as can be seen in Figure 9, whereas in run 6, the water supply rate changed from a lower value to a higher value and then back to the lower value as in Figure 10. The bed and water levels were monitored at regular intervals of time. The figures 11a to 11f show the bed and water levels at the instants, A, B, C, D and E identified in Figure 9 for run 5. The continuous lines are the measured water and bed levels whereas the dots are the predicted values using the mathematical model. From these figures, it can be seen that the model predictions agree reasonably well with the experimental measurements. Similar agreement was noticed for run 6 as well. (The figures corresponding to run 6 are not shown here). In these runs, both degradation and aggradation processes were present.

In all the runs reported here, the channel bed was covered with dunes as can be seen from the figures depicting the water and bed levels. No attempt was made to compute the mean bed and water levels from the measured data. But a visual examination of the figures shows that the measured bed and water levels are distributed around the predicted mean values.

Even though the model predictions were not made for the dune shapes and their movement, their effects were taken into consideration in computing

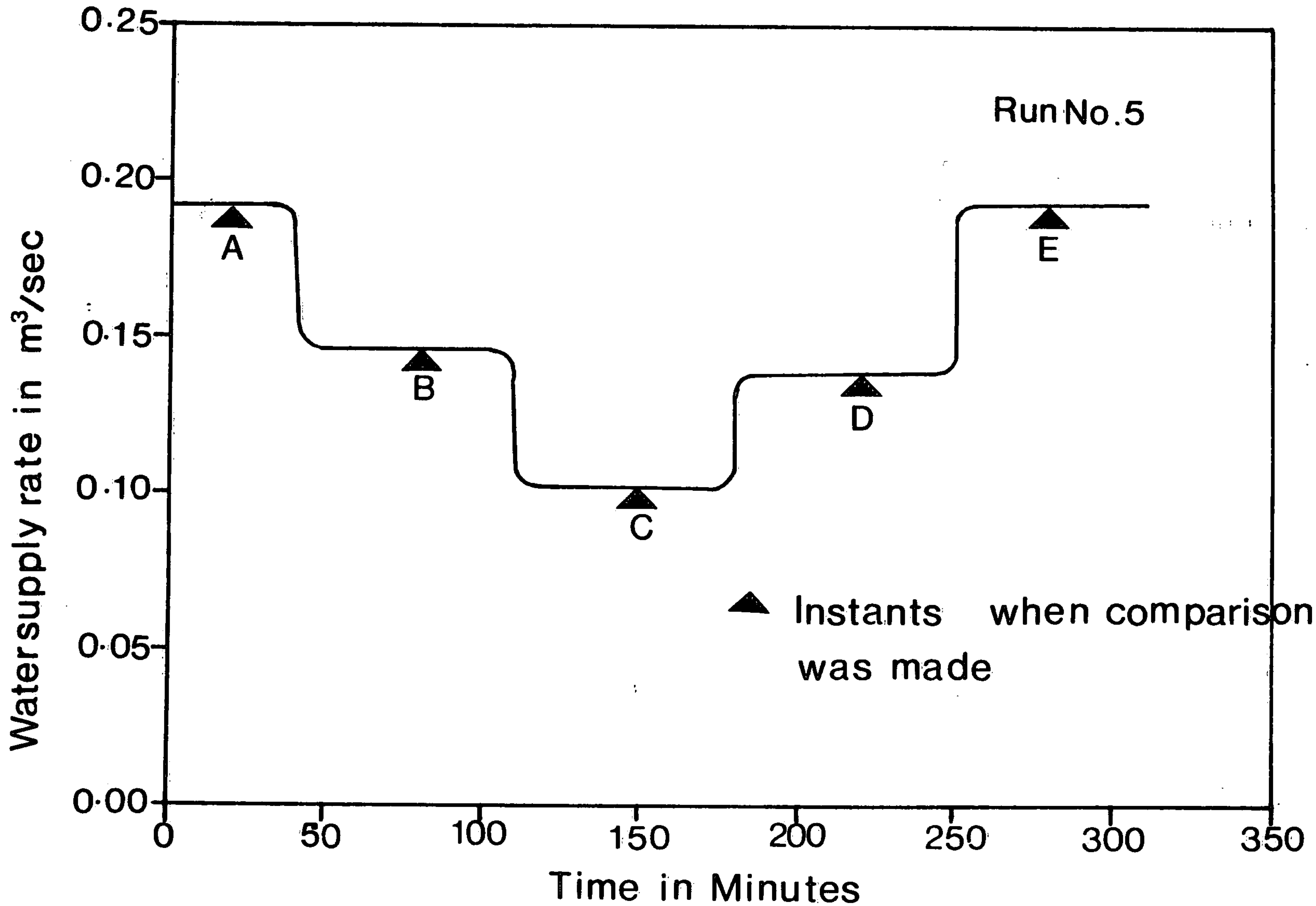

Fig. 9. Variation of water supply rate at flume entrance as a function of time

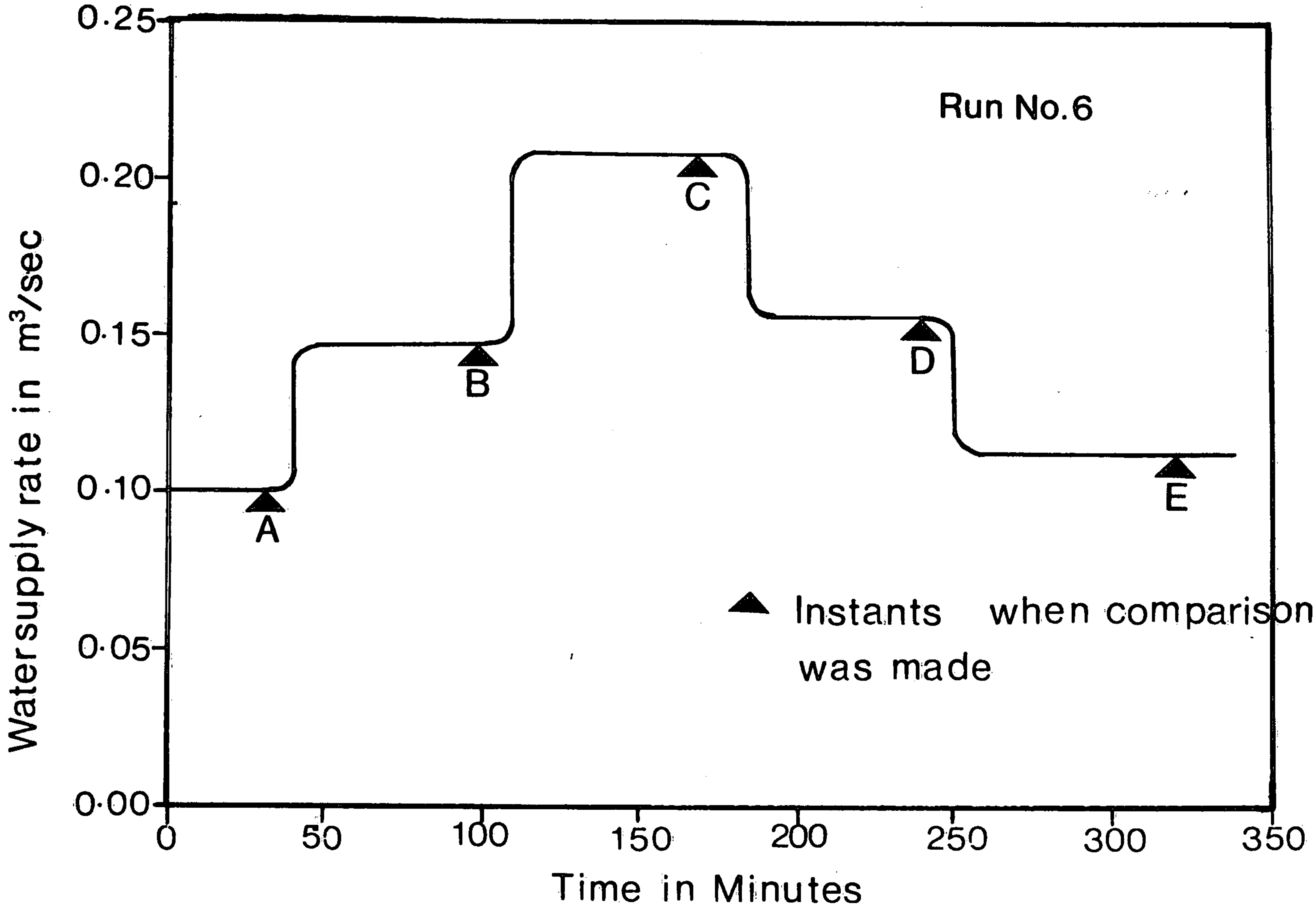

Fig. 10. Variation of water supply rate at flume entrance as a function of time

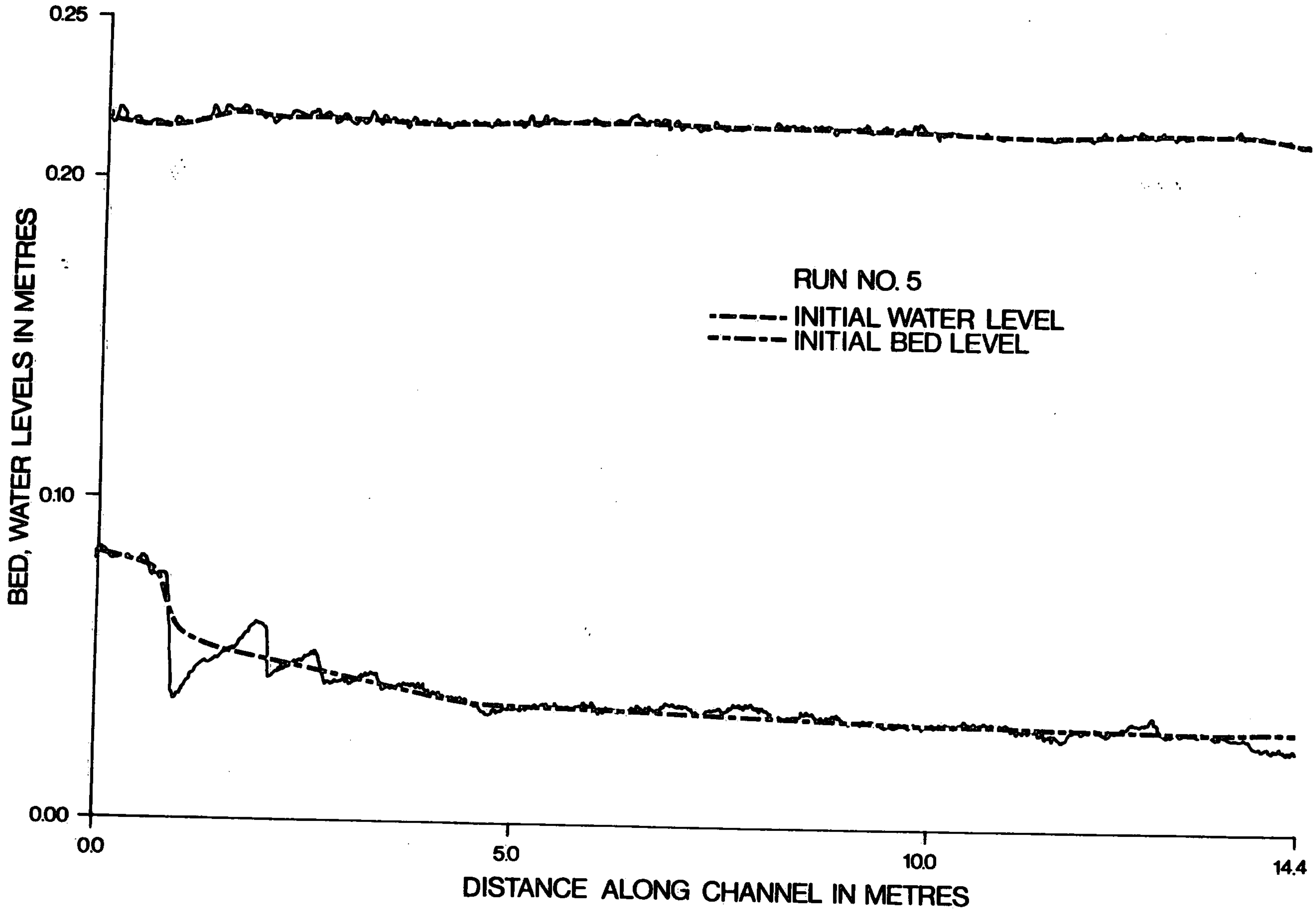

FIGURE 11a. COMPARISON OF MODEL PREDICTIONS WITH LABORATORY MEASUREMENTS

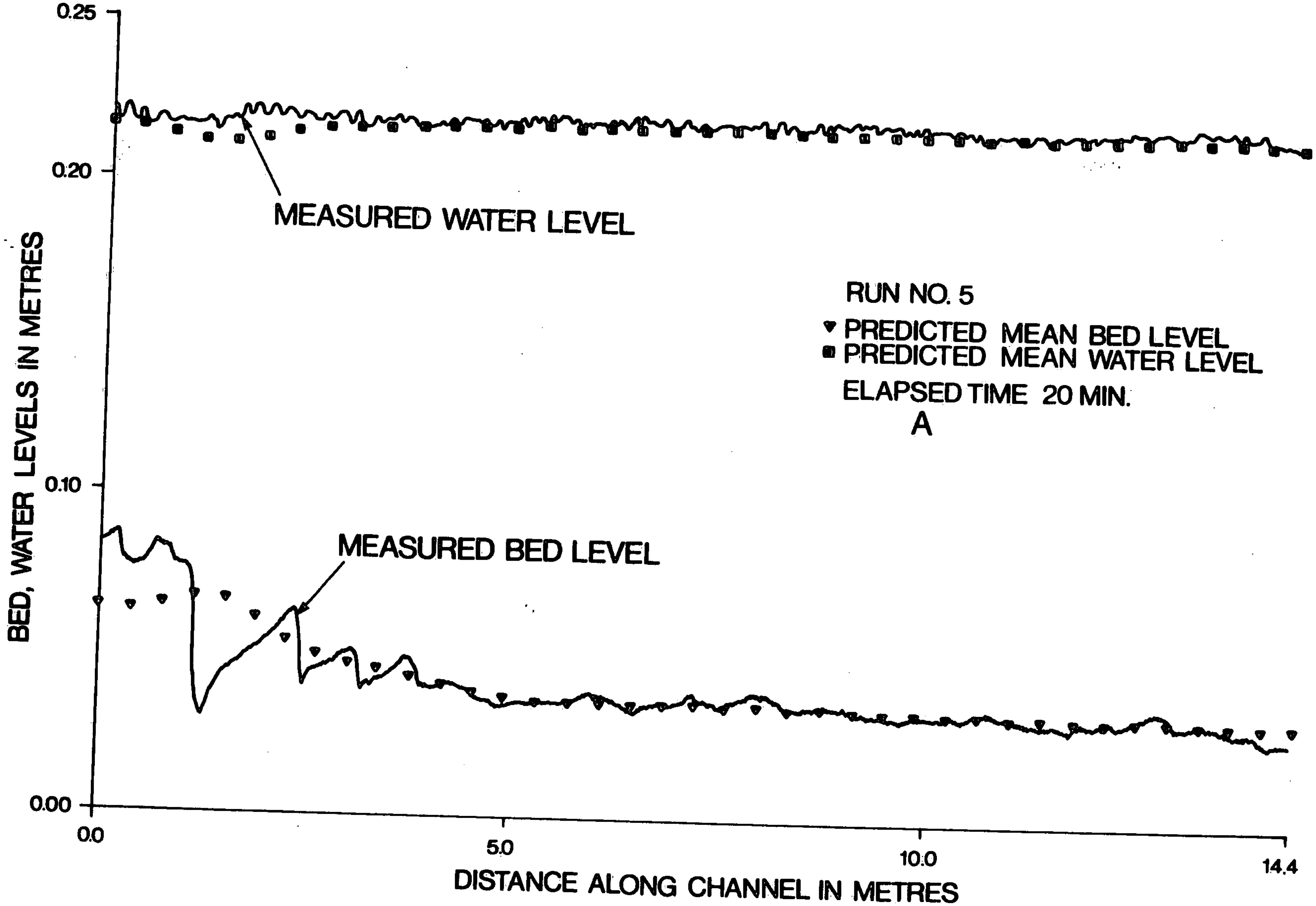

FIGURE 11b. COMPARISON OF MODEL PREDICTIONS WITH LABORATORY MEASUREMENTS

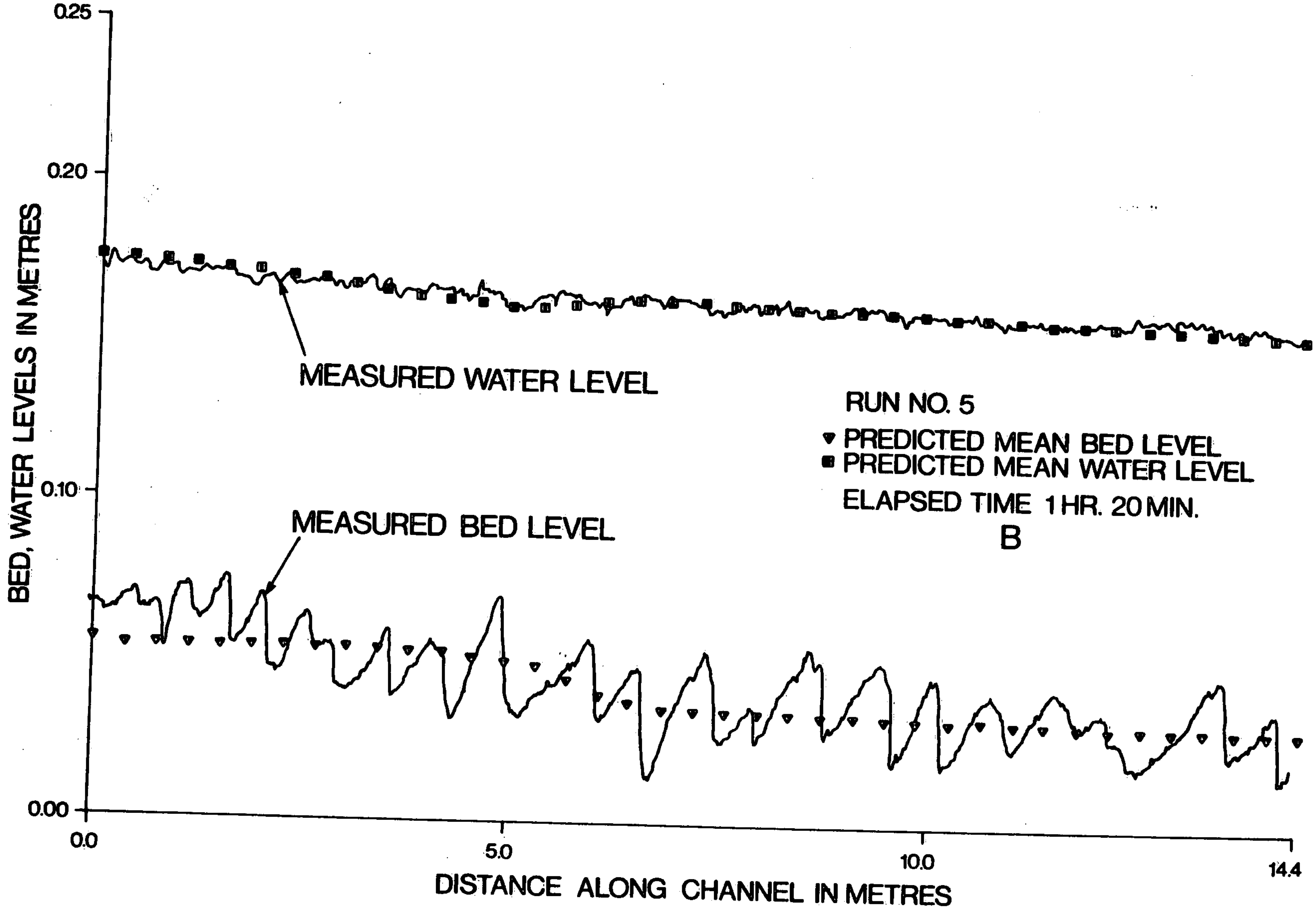

FIGURE 11c. COMPARISON OF MODEL PREDICTIONS WITH LABORATORY MEASUREMENTS

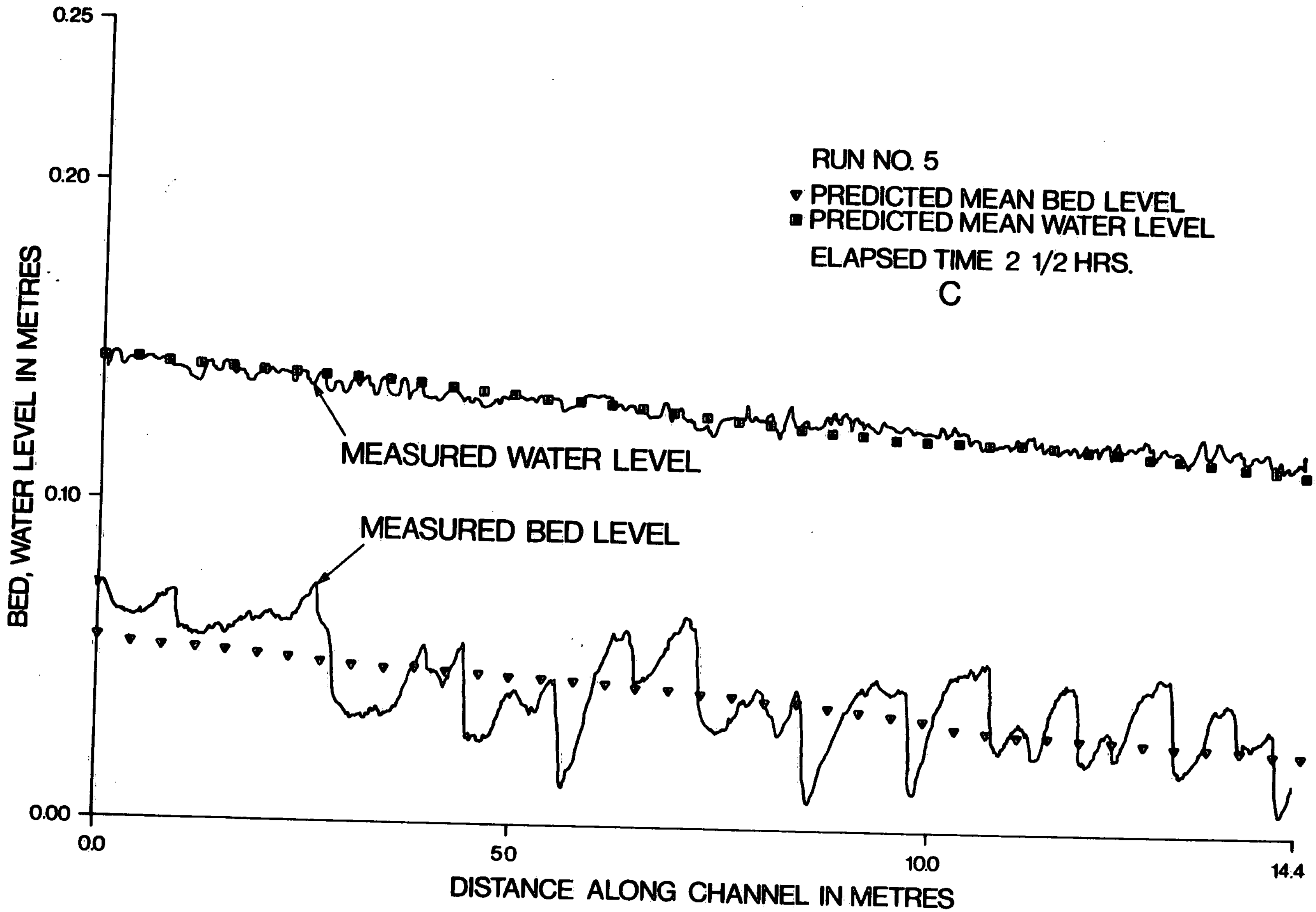

FIGURE 11d. COMPARISON OF MODEL PREDICTIONS WITH LABORATORY MEASUREMENTS

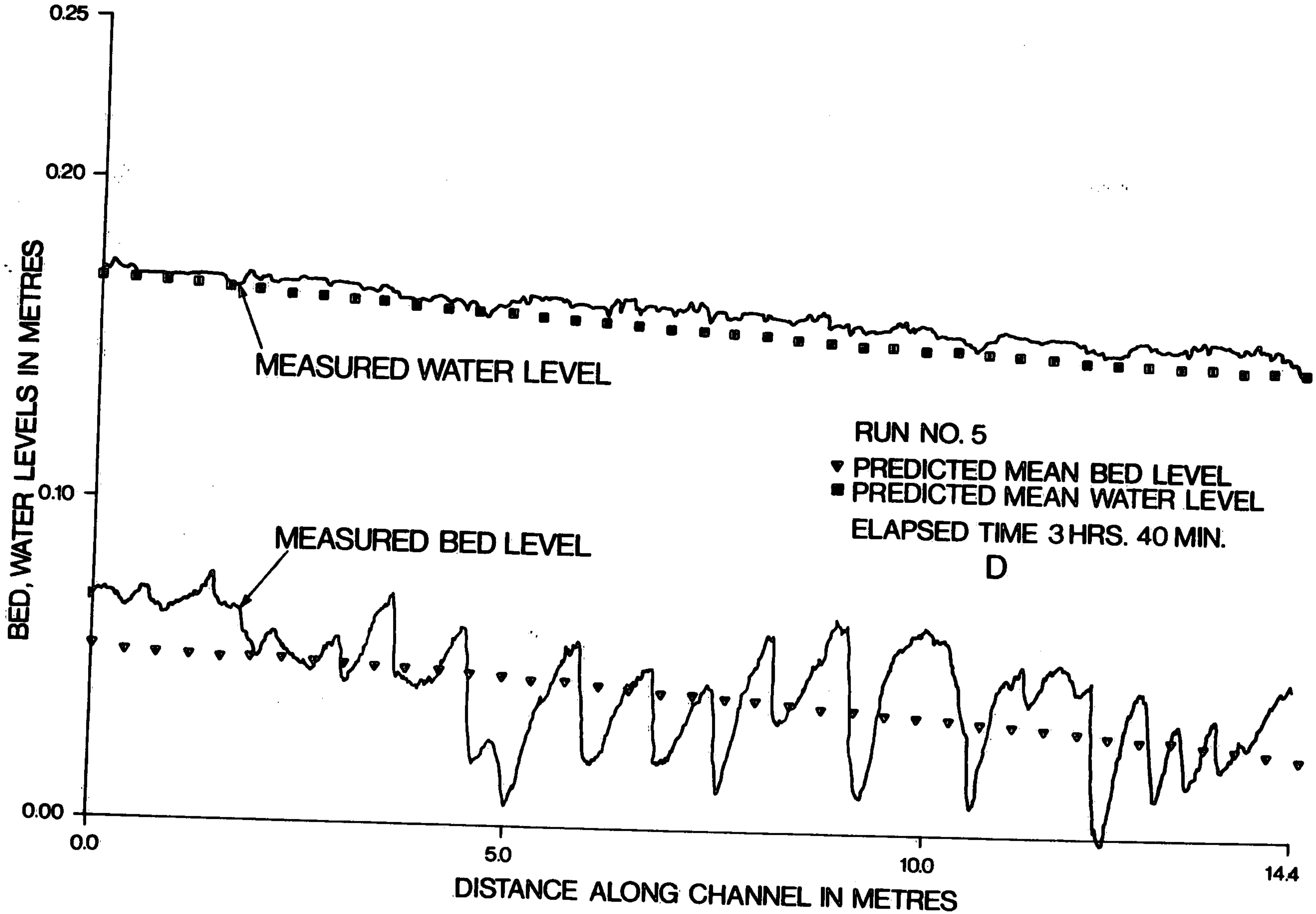

FIGURE 11e COMPARISON OF MODEL PREDICTIONS WITH LABORATORY MEASUREMENTS

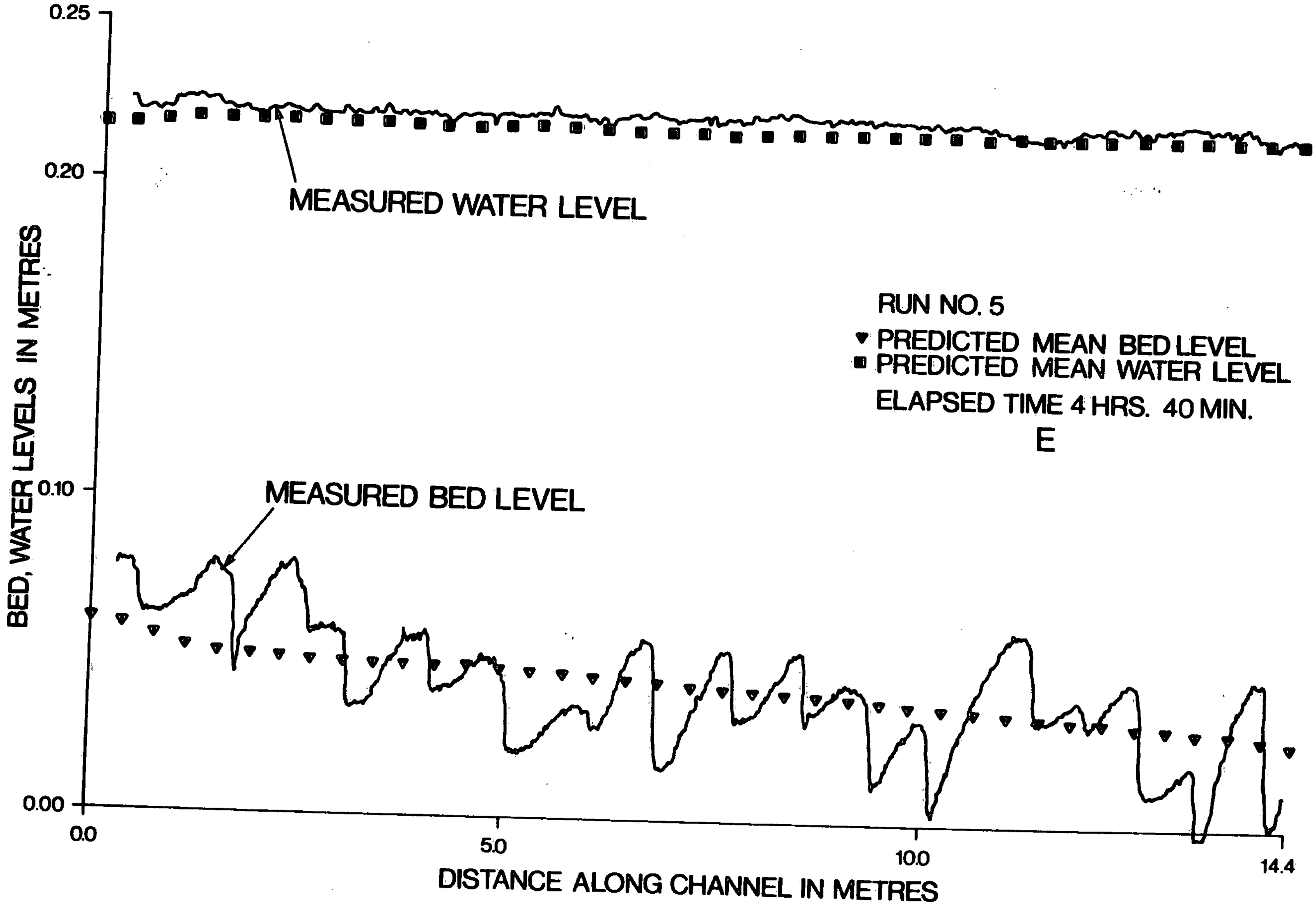

FIGURE 11f. COMPARISON OF MODEL PREDICTIONS WITH LABORATORY MEASUREMENTS

the friction parameters using the formulae of Kishi and Kuroki. The model, however, is capable of predicting the dune movement. For such an application, the sediment transport function has to be such that it reflects the variation of the sediment transport rate over the length of a dune. Recently V. M. Ponce, J. L. Garcia and D. B. Simons (13) have presented a model to predict the alluvial bed transients by considering only the sediment continuity equation and the momentum equation. They used an empirical power relation for the sediment transport rate. More work is needed to establish an equation reflecting the true variation of the sediment transport rate over the length of a sand wave.

5.0 SUMMARY AND CONCLUSIONS

A mathematical model is described to predict the mean bed level, water level and discharge as functions of time and distance along the channel for time-dependent flow rate and sediment input rate at the upstream. The model uses the friction factor relations developed by Kishi and Kuroki which take into account the various bed forms that could be found in natural streams. The sediment transport relation developed by Ackers and White which was found to be superior to most of the available relations was adopted in this model.

The model was verified in a laboratory channel by simulating various sedimentation processes such as aggradation and degradation. The experimental measurements indicate that the model is capable of predicting the mean bed and water levels in mobile boundary channels with reasonable accuracy.

Unlike some previous models, the application of this model does not require the model calibration since all the coefficients appearing in the model are predictable from the initial conditions.

6.0 ACKNOWLEDGEMENTS

The author wishes to thank Dr. T. M. Dick, the chief of the Hydraulics Research Division and Dr. Y. L. Lau, the head of the Environmental Hydraulics Section of the Hydraulics Research Division, for reviewing the manuscript and providing valuable suggestions. The author also wishes to thank Mr. J. Heidt, the research technician, for carrying out the experiments and Mrs. E. J. Jones for typing the manuscript.

APPENDIX I - REFERENCES

1. Ackers, P. and White, W. R., "Sediment Transport: New Approach and Analysis", Journal of the Hydrualics Division, Proc. ASCE, Vol. 99, No. HY11, Nov. 1973.

2. Bhamidipaty, S. and Shen,H. W., "Laboratory Study of Degradation and Aggradation", Journal of the Waterways, Harbors and Coastal Engineering Division, Proc. ASCE, Vol. 97, No. WN4, Nov. 1971.

3. Chen, Y. H. and Simons, D. B., "Mathematical Modelling of Alluvial Channels", Vol. 1, Symposium on Modelling Techniques, San Francisco, California, Sept. 1975.

4. Chen, Y. H., "Mathematical Modelling of Water and Sediment Routing in Natural Channels", Ph.D. Thesis, Colorado State University, 1973.

5. Cunge, J. A. and Perdreau, N., "Mobile Bed Fluvial Mathematical Models", La Houille Blanche, No. 7, 1973.

6. Cunge, J. A. and Simons, D. B., Mathematical Model of Unsteady Flow in Moveable Bed Rivers with Alluvial Channel Resistance", XVIth Congress of the International Association for Hydraulic Research, São Paulo, Brazil, 1975.

7. Cunge, J. A. and Liggett, J. A., "Numerical Methods of Solution of Unsteady Flow Equations", Chapter 4, Unsteady Flow in Open Channels, Vol. 1, edited by K. Mahmood and V. Yevjevich, Water Resources Publications, 1975.

8. Einstein, H. A., "The Bed-Load Function for Sediment Transportation in Open-Channel Flows", U.S. Dept. of Agriculture, Technical Bulletin No. 1026, 1950.

9. Engelund, F. and Hansen, E., "A Monograph on Sediment Transport in Alluvial Streams", Teknisk Forlag, Copenhagen, 1967.

10. "The Bed Configuration and Roughness of Alluvial Streams", by Task Committee on Bed Configuration and Hydraulic Resistance of Alluvial Streams, Committee on Hydraulics and Hydraulic Engineering, The Japan Society of Civil Engineers, Nov. 1974.

11. Krishnappan, B. G. and Snider, N., "Mathematical Modelling of Sediment Laden Flows in Natural Streams", Scientific Series No. 81, Inland Waters Directorate, CCIW, Burlington, Ontario, 1977.

12. Meyer-Peter, E. and Müller, R., "Eine Formel zur Berechnung des Geschiebetriebes", Schweiz. Bauzeitung, 67 jg., Zurich, 1949.

13. Ponce, V. M., Garcia, J. L. and Simons, D. B., "Modelling Alluvial Channel Bed Transients", Journal of the Hydraulics Division, ASCE, Vol. 105, No. HY3, March 1979.

14. Preissmann, A., "Propagation des instrumescences dans les canaux et rivières", 1re Congrès de l'Association française de calcul, Grenoble, 1961.

15. Toffaleti, F. B., "Definitive Computation of Sand Discharge in Rivers", Journal of the Hydraulics Division, ASCE, Vol. 95, No. HY1, Jan. 1969.

16. White, W. R., Milli, H. and Crabbe, A. D., "Sediment Transport Theories - A Review", Proc. Inst. Civ. Engg., Part 2, Vol. 59, June 1975.

APPENDIX II - NOTATION

The following symbols are used in this paper.

x = co-ordinate axis along the length of a stream

η = vertical co-ordinate measured from the mean bed level

z = vertical distance between a fixed datum and the mean bed level

y = flow depth

t = time

g = acceleration due to gravity

Q_s = volumetric sediment transport rate

q_s = lateral sediment input rate

Q = flow rate

q = lateral inflow rate

P = wetted perimeter

B = top width

A = flow cross-sectional area

R = hydraulic radius

A_x^η = rate of change of A with respect to x when η is held constant

S_o = slope of the river bed

S_f = slope of the energy grade line

p = volume of sediment on the bed per unit volume of bed layer

C_{av} = average volumetric sediment concentration

v = average flow velocity

v_* = sheer velocity

C = v/v_*: friction coefficient

D_{50} = median sediment size

γ = specific weight of water

γ_s = submerged specific weight of sediment

Y,Z, Fr = dimensionless groups

const, m, n = friction parameters